A DISSERTATION REPORT

on

Effect of Tool Radius and Iso-parametric Discretization of Triangulated NURBS Surfaces on Surface Finish in 3-axis Vertical Finish Machining Using Ball End Mill

Submitted in partial fulfilment of the requirements for the award of degree of

Master of Engineering

in

CAD/CAM Engineering

Submitted by:

PRAKHAR JAIN
Roll No: 801481017

Under the guidance of

Dr, Ravinder Kumar Duvedi
Assisstant Professor

MECHANICAL ENGINEERING DEPARTMENT

THAPAR UNIVERSITY, PATIALA-147004, INDIA

JULY-2016

Declaration

I hereby declare that work done in this thesis entitled, "**Effect of Tool Radius and Iso-parametric Discretization of Triangulated NURBS Surfaces on Surface Finish in 3-axis Vertical Finish Machining Using Ball End Mill**" " is an genuine record of my own work carried out in completing the thesis requirement for the degree of **Master of Engineering in CAD/CAM Engineering** at Thapar University, Patiala, under the guidance of Dr. Ravinder Kumar Duvedi, Assisstant Professor, Mechanical Engineering Department, Thapar University, Patiala

This matter embodied in this report has not been submitted in part or full to any other university or institute for the award of any degree.

Prakhar Jain

Prakhar Jain

(801481017)

This is to certify that above declaration made by the student concerned is correct to the best of our knowledge and belief.

Dr. Ravinder Kumar Duvedi

Assistant Professor

Department of Mechanical Engineering

Thapar University, Patiala

Countersigned by:

Dr. S.K. Mohapatra
Senior Professor and Head
Mechanical Engineering Department
Thapar University, Patiala

Dr. S.S. Bhatia
Dean of Academic Affairs
Thapar University, Patiala

Acknowledgement

I am truly and deeply thankful to my mentor, Dr. Ravinder Kumar Duvedi for the amount of knowledge that he shared with me, along with the countless amounts of time that he spent for me. The enthusiasm and effort that he had put into this topic and to make me better off will always be remembered. I heartily thank him, for offering me this wonderful opportunity. Without his guidance and persistent help, this thesis would not have been possible. For all his help and guidance throughout the years, I am indebted to him.

I thank the entire faculty and staff of Mechanical Engieering Department, Thapar University, for their help and moral support.

I also acknowledges the use of facilities of State Initiated Design Centre (SIDC) for woodworking of Mechanical Engineering Department, Thapar University, Patiala, set up under financial support from Handicrafts Division of Ministry of Textile, Government of India

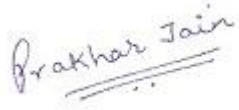

Prakhar Jain

Abstract

The precision machining of sculptured surfaces is a challenge. The modern CAD-CAM technology has been explored tremendously for adding ease of machining complex sculptured shapes and indeed these systems has added to the productivity of the modern shop floor. The choice of the proper CNC machining centre, the geometry of the cutting tools, the accurate 3D representation of CAD geometry of the part to be machined and the selection of proper NC toolpath computation algorithm are the key components that counts for successful output which in this case is error free and faster machining of complex surfaces within the required surface finish.

For the given input machining conditions the accuracy of the toolpath data greatly influence the quality of the machined surface. The use of ball end milling cutter is preferred for sculptured surface machining. The computation of toolpath data for a ball end mill is well established and it is also a known fact that the use of 3D part data in the triangulated faceted format eases the computation involved for determination of gouge-free toolpath data for CNC machining. Though NURBS surfaces can be used to accurately define the geometric information of the 3D surface models, but it is a challenge to determine the gouge free tool positioning data directly from NURBS surfaces. In many applications the NURBS surfaces are preferred for solid modelling and part representation, but for manufacturing applications the use of triangulated data models can yield gouge-free machining results.

Thus, in this work a generalized NURBS code is used to fit a NURBS surface through a given set of data points. Also, the developed NURBS code is used to extract geometric information of the developed NURBS surface in the form of a uniform grid of iso-parametrically located points. The iso-parametric point cloud data is intern used to define a triangulated meshed surface which is further used to generate the gouge-free toolpath data for a ball end milling cutter. The toolpath generation algorithm used for toolpath computation for ball end milling cutter uses the concept of "*drop the tool*" and "*ray tracing algorithm*" in a unique way which ensures that the user defined scallop height is achieved by computing the adaptive side-step values for various machining passes for a zig-zag toolpath pattern with a uniform feed forward spacing of tool motion. In this work the mathematical model used for development of this algorithm is presented along with the validation of the results from the developed algorithm for faceted freeform, concave and convex surfaces. Further this algorithm is used to identify the relationship between the tool dimensions, iso-parametric triangulation of NURBS surfaces and

the surface finish that can be achieved within a reasonable number of machining passes. The results from the algorithm shows that the smaller tool radius helps achieve lower scallop heights while the change in iso-parametric spacing for triangulated meshing of the NURBS surface does not play a role in reducing the scallop height when subjected to a condition that a minimum side-step value has to be ensured to keep the maximum number of tool passes in overall toolpath data under control. The overall procedure of the developed toolpath algorithm for triangulated NURBS surface models is presented in this thesis work along with results obtained for various analytical simulation studied during this work.

Contents

List of Figures

List of Tables

Nomenclature

C_c	Cutter contact point
C_l	Cutter location point
u, v, s, t	Parameters varying from 0 to 1
Δu	Step size for parameter u
Δv	Step size for parameter v
$\hat{N}$	Normal vector
T_1	Initial tool position
T_2	Final tool position
P_1, P_2, P_3, P_4	Vertices of triangle/ Tool location points
P_5 and P_6	Tool location points
r	Radius of ball end mill
I_c	Intersection points of two spheres
$\hat{u}$, $\hat{v}$, $\hat{w}$	Direction vectors
M	Midpoint of two cutter locations on neighbouring tool paths
u	Wind speed
S_s	Side step value
I_{stl}	Intersection point on STL surface
h	Scallop height (Distance between I_c and I_{stl})
F_s	Forward step value
S_{sl}	Side step value
S_{si}	Side step initial value
S_{sr}	Side step right value
ε	User defined scallop value

Acronyms

2D	Two Dimensional
3D	Three Dimensional
ASCII	American Standard Code for Information Interchange
CAD	Computer Aided Design
CAM	Computer Aided Manufacturing
CL	Cutter location
CNC	Computer Numeric Control
STL	Stereo Lithography
APT	Automatically Programmable Tool
NURBS	Non Uniform Rational B Splines
FFRNS	Freeform Reference NURBS Surface
FFSTLS	Freeform STL Surface
FFOBJS	Freeform Object Surface
CCRNS	Concave Reference NURBS Surface
CCSTLS	Concave STL Surface
CCOBJS	Concave Object Surface
CVRNS	Convex Reference NURBS Surface
CVSTLS	Convex STL Surface
CVOBJS	Convex Object Surface

Chapter 1 Introduction

Precision machining of sculptured surfaces is a complicated task and for this CNC machining centres are used. Sculptured surfaces are either defined mathematically or by reverse engineering and there is a need to convert them to a data format that can be useful for NC toolpath generation. The NC toolpaths generated from custom algorithms which are also known as CAM algorithms are used to run the drives of CNC machining centres for relative position of cutting tool with respect to part surface. Thus it is important that the algorithm that is used for toolpath generation must be very accurate in terms of tool positioning with respect to surface geometry of the part to be machined. The machined surface is generally checked for its accuracy by the surface finish generated it. For machining of sculptured surfaces, ball end milling cutter is very commonly used. It has been found from literature that triangulated surface offer computational efficiency for NC toolpath generation. While, at the same time, mathematically correct representation of sculptured surfaces can be defined using the NURBS surfaces. Thus in this dissertation work, an attempt has been made to generate NURBS surface from given data points which are intern used to generate point cloud data on the defined NURBS surface. This point cloud data is further used for the generation of triangulated mesh for that NURBS surface. The triangulated mesh surface is then used to generate NC toolpath data for ball end milling cutter by considering the fact that user defined scallop height must be maintained between the consecutive machining passes. Finally, the results for the various machined parts chosen which are namely freeform surface, concave surface and convex surface has been derived and are discussed in the subsequent chapters. Various aspects of sculptured surfaces, NURBS modelling, benefits derived from triangulated meshes for generation of NC toolpath data and advantages of using ball end mill as well as other associated aspects are discussed in the subsequent sections.

1.1 Sculptured Surfaces

Sculptured surfaces are used in geometric modelling of complex parts that can't be described by simple curved surfaces [1]. The definition is intuitive rather than formal. They further can be categorized as composite parametric and reverse engineered surface.

1.1.1 Sculptured surface as composite parametric surface

Composite parametric surface are composed of different rational patches like NURBS, Bezier and B-spline interconnected to each other by different continuity. Each of the surface patches is defined mathematically. These mathematical surface patches are either analytical patches or synthetic patches. Analytical patches include planar surfaces, ruled, tabulated and surface of revolution. Synthetic surface include Hermite, Bezier, B-spline, Triangular coons patch and NURBS.

1.1.2 Sculptured surfaces as reverse engineered surface

Reverse engineered surfaces are generated from point cloud data by 3-D scanning of manually cladded or clay molded surfaces. They can be represented by either by point cloud, triangulation or by a mathematical model.

1.2 Machining of Sculptured Surfaces

Sculptured surfaces are machined by using CNC machines owing to the fact that it provides better surface finish in less machining time. Machining can be done by 3, 4 and 5-axis CNC machine tools. But, 3-axis CNC machine tools are widely used. For machining the surface, toolpath is required to guide the tool along the prescribed path in order to achieve desired accuracy. For this purpose, planning of the toolpath becomes crucial as it is an important aspect in the machining of sculptured surfaces. A toolpath generation problem can be categorised into three stages such as specifying the toolpath planning technique and toolpath footprint pattern, specifying tool positioning strategy and selecting proper tool shape. Different types of input are considered for toolpath generation such as cloud of points, faceted model and CAD model but faceted or polyhedral model are mostly preferred because of simplified calculations involved. In present work, triangulated model for the generation of toolpath footprint is used.

1.3 Toolpath Planning for Sculptured Surfaces

There are different types of 3-axis toolpath planning techniques directly from polyhedral model. Iso-parametric and iso-planar approaches are usually adopted for toolpath planning. In iso-parametric approach, CC points are created in the direction of one parameter while keeping the other one constant. But, the disadvantage with iso parametric approach is that the constant spacing in the parametric domain leads to non-uniform spacing in Cartesian space that creates unevenly distributed scallops which could affect the accuracy. In Iso-planar approach series of parallel planes are used to cut the surface to be machined. The point of intersection of the

surface and the cutting planes gives the CC points from where the CL points could be determined based on the milling cutter used for the machining. It gives poor machining efficiency and surface finish when used with irregular profiles. Iso-scallop method provides constant scallop height throughout the surface. Different toolpath topologies are implemented now days by researchers such as Direction parallel, contour offset and space filling curves (SFC) but zig-zag toolpath footprint also known as direction parallel is known for better cutting loads during machining. Current work incorporates controlled scallop height toolpath planning approach by using zig-zag toolpath footprint topology.

Toolpath generation depends greatly on the tool shape utilized for machining. When the surface to be machined is flat then flat end mills are mostly preferred as the profile of the tool exactly matches the surface. For the curved surface, industries prefer ball end mill because it simplifies the task of toolpath creation. Radiused end mill enjoys the advantage of both flat and ball end mill and is becoming increasingly popular. Present work employs ball end mill for the machining purpose as it's easy to position onto the desired surface and the calculation for the CL points becomes relatively simple and fast. Also, ball end mill provides greater surface finish when there is an abrupt change in the curvature [25]. Figure 1.1 shows shape of ball nosed milling cutter.

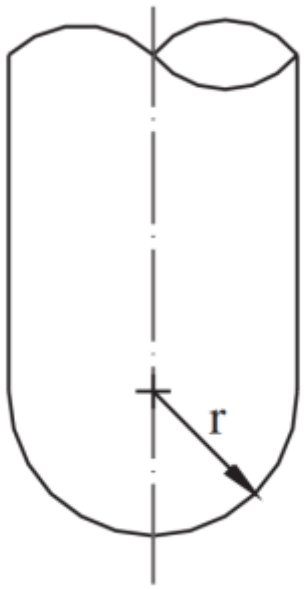

Figure 1.1: Ball nose end mill

CNC machining can be categorised into the following phases namely Roughing, Semi finishing, finishing and clean-up. A large part of material removal takes place during the roughing stage which approximates the surface to the desired profile. Semi finishing operations

removes the shoulders left during the first stage followed by finishing where the surface is given the precise shape. During the cleaning up stage, the uncut portion left during the finishing stage is sheared off because of the usage the cutter of greater radius. Focus in the present work is on the creation of finishing toolpath.

1.4 Cutter Contact and Cutter Location Points

The CC point is the point on the toolpath which involves a direct contact of the tool with the work piece. The CL point is a stationary point which allows controller to drive the tool through them along the prescribed toolpath. CC points are not considered as the reference points for the tool to track because they are not bound to be located at the centre of the cutter. On the other hand, the CL points lies along the perpendicular direction of the respective cutter contact point. CL is obtained from CC points and from and along surface normal. Therefore, CL points are considered as the reference coordinate points for the tool to track on. CL point is located at the centre of ball end milling cutter. Figure. 1.3 depicts CL and CC points.

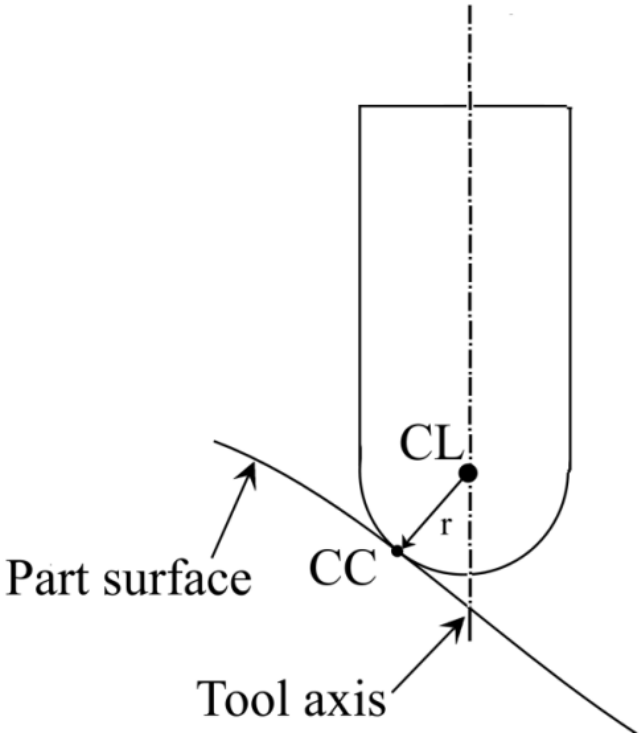

Figure 1.2: Cutter contact and cutter location points for ball end mill

The CL points for different milling tool shapes are shown in the figure below:

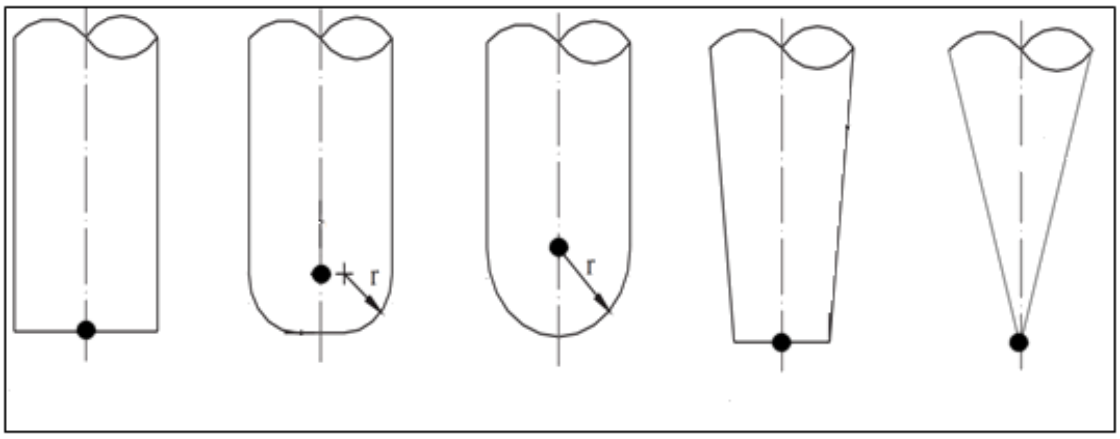

Figure 1.3: CL points for milling tool shapes

1.5 Scallop Height Control

Scallop height is defined as the height of the uncut material left when the tool moves in the cross feed direction. It is measured normal to the part surface to be machined. Scallop height direct affects the surface finish of the part. It is required to be minimised because smaller is the height of the scallop better is the surface finish. Also, the polishing time post machining becomes minimised along with the reduction of errors. Hence, side step distance is required to be adjusted as they are the reason for the formation of scallops. Figure 1.4 denotes the direction where the scallop height is required to be calculated and Fig. 1.5 denotes zig-zag toolpath footprint along with feed forward and side step interval.

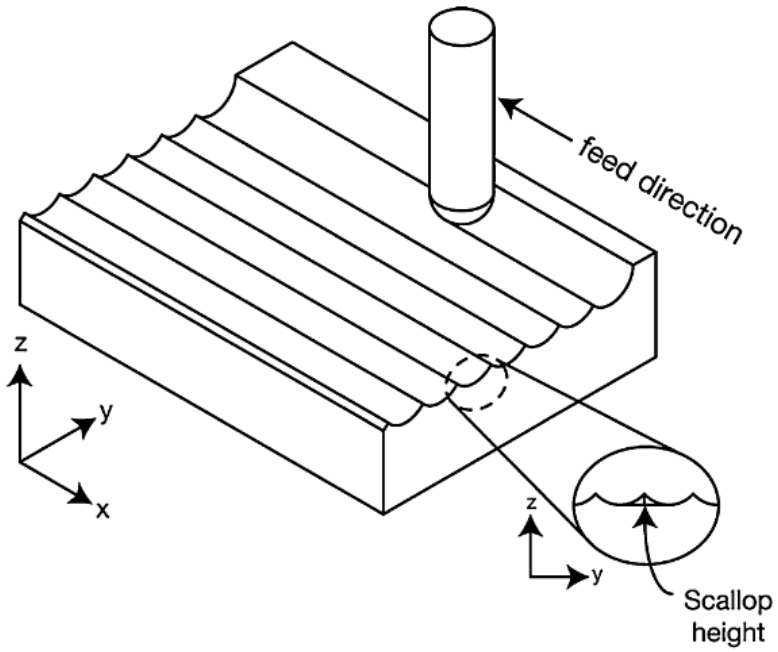

Figure 1.4: Direction of scallop height calculation [25]

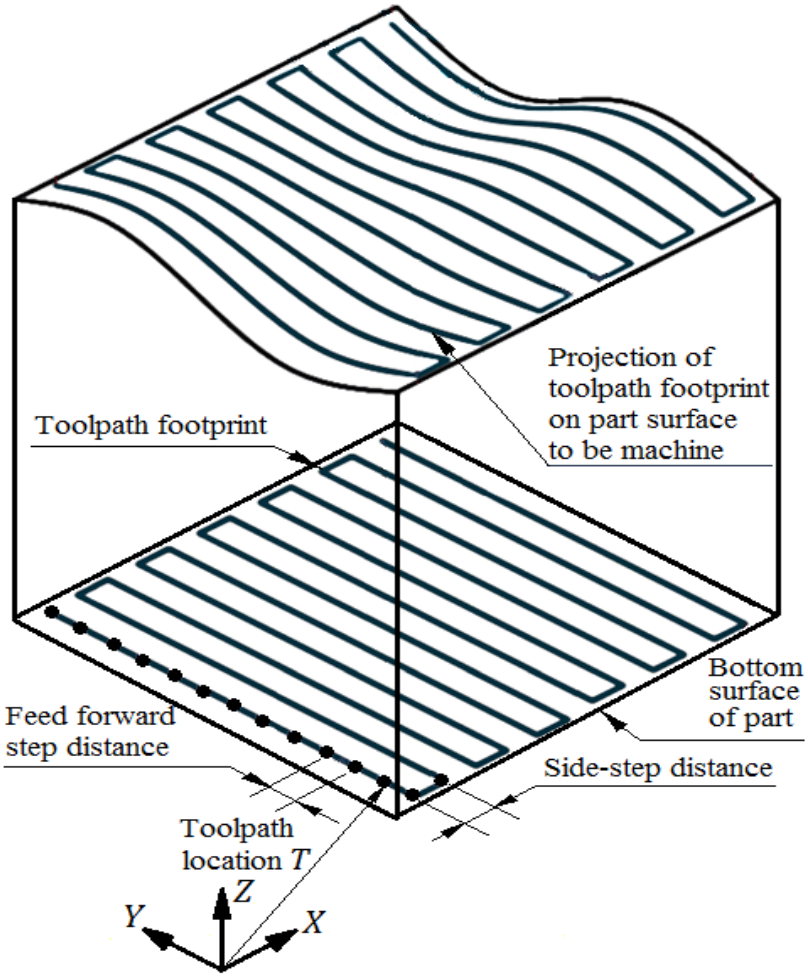

Figure 1.5: Feed forward and side step distance for zig-zag toolpath footprint [28]

1.6 NURBS surface as triangulated mesh

Non Uniform Rational B-Spline surface (NURBS) is used to define smooth curves and surfaces. It's a unified mathematical model which is a function of couple of parameters that maps in a 3D space. It is widely used in the representation of freeform curves and surfaces. The major advantage of using NURBS is that it allows the user to assign weights to each of the control point and thereby allowing user to control the behaviour of a geometric shape.

Toolpaths generated directly from NURBS design surface are poor in accuracy and contains lot of geometric errors. The major problem of using NURBS directly is that tool penetrating the surface during the machining resulting in gouges and uneven scallops. Hence, to achieve greater computational efficiency and gouge free machined surface, triangulation of NURBS surface is done and toolpaths are then planned for this triangulated mesh.

1.7 Present Work

In present work, a generalized NURBS code is used to fit a NURBS surface through a given set of data points and to extract geometric information of the developed surface in the form of a uniform grid of iso-parametrically located points. Polyhedral model from this iso-parametric point cloud data is used to define a triangulated meshed surface which is further used to generate the gouge-free toolpath data for a ball end milling cutter. The controlled scallop height toolpath generation algorithm is used for the computation of toolpath data with ball end milling cutter by using the concept of "*drop the tool*" and "*ray tracing algorithm*" in such a way that the user defined scallop height is achieved by computing the adaptive side-step values for various machining passes for a zig-zag toolpath pattern with a uniform feed forward spacing of tool motion. In this work, the mathematical model used for development of this algorithm is presented along with the validation for faceted freeform, concave and convex surfaces. Further, this algorithm is used to identify the relationship between the tool dimensions, iso-parametric triangulation of NURBS surfaces and the surface finish that can be achieved within the reasonable number of machining passes.

Chapter 2 Literature Review

In this dissertation work, an attempt is made to generate 3-axis NC toolpath for NURBS surface by triangulation of iso-parametrically discretized point cloud data. Toolpath is generated in such a way that the scallop height between the consecutive machining passes remains within the range specified by user. A study to identify the relationship between the tool dimensions, iso-parametric discretization of triangulated NURBS surfaces and the surface finish that can be achieved within the reasonable number of machining passes is done. For this purpose, study of the machining of sculptured surface, toolpath generation methods, toolpath positioning strategies, study of various path topology and parameters and study of the effect of tool shape on surface to be machined is done. Toolpath planning process for sculptured surface can be categorized into following subcategories with specific cutter shape [1], defining the toolpath pattern and path direction [2] defining the points which are to be tracked by tool [3] checking the local and global gouging of the tool with the surface [22]. Thus, a method that optimizes the above mentioned criteria is always required.

2.1 Toolpath Topology and Path Parameters

A proper toolpath could be established by defining path topology and path parameter. Path topology is the pattern with which the tool links the arrangement of CC points in order to approximate sculptured surface. Generation of each toolpath is led by proper selection of path topology and path parameters. Shortest path length and minimum tool retractions can be achieved by selecting the appropriate topology. Contour parallel and direction parallel paths are generally used for milling of sculptured surface and for clean-up surfaces strip normal and parallel paths are mostly used. Path parameters such as side step and feed forward step must be defined appropriately before being incorporated in the toolpath. The distance between two consecutive cutter contact points is known as forward step and sidestep is the distance between two adjacent paths as shown in Fig1.5. A toolpath is thus created by defining proper topology and parameters. It should be evaluated by following three criteria- Quality, efficiency and robustness [22].

2.2 Toolpath generation techniques

Toolpath generation techniques based on CC and CL points are discussed below.

2.2.1 Cutter contact based methods

In this method, the toolpath is generated by joining the CC points and then the CL points are obtained from the respective CC points. Toolpath is generated by joining the CL points.CC based toolpaths are parametric, drive surface and guide plane method. The parametric method is an approach that involves creation of the tool paths in parametric domain. The iso-parametric method is one such approach. In this methodology, toolpaths are generated along the direction of one parameter while keeping the other parameter constant. The benefit it is that the surface data could be directly utilised in toolpath generation. Linear entity in this domain is actually nonlinear in other which is shown in Fig 2.2. Therefore, iso-scallop method [1–3] was proposed to overcome the disadvantage of the above approach. The height of the scallops is kept constant in this approach.

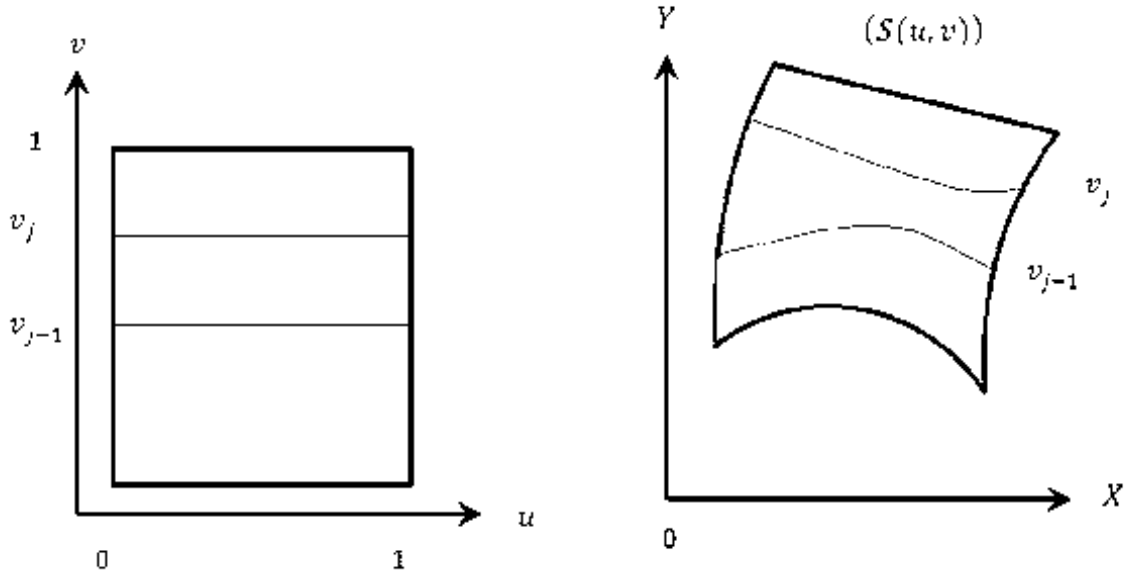

Figure 2.1: Design surface in (a) parametric and (b) cartesian domain

In drive surface approach, toolpath is generated by cutting the surface with the series of parallel planes. The intersection points are the desired CC points. The CL points are thus calculated based on the tool shape used. The major disadvantage of using the method is in the selection of the distance between the cutting planes. In order to simplify the calculations, vertical and horizontal planes are used .This approach is also known as iso-planar method.

In guide plane method, toolpath is generation in two steps. First; the planning of the toolpath is done on the guide plane .Second; the planned toolpaths are then projected on to the offset surface. This approach also bears the similar drawback as to the iso-planar. There still occurs the problem of choosing the distance between the toolpath. This leads to poor surface finish and lower machining efficiency. An approach was presented to counter the disadvantage of the above methods. The guide surface is approximated to the design surface [7]. However, the problem of grid accuracy still occurs.

2.2.2 Cutter location based methods

In this method, CL points are directly determined and are approximated to produce toolpath. The offset surface is used as the medium of CL point generation. In present work tool drop method suggested by Manos et al.[14] is used to generate CL points. The CL points are then joined to produce gouge free toolpath.

2.3 Tool Path Generation Based on Point Cloud Data

Kim et al.[6] presented the approach for generating toolpaths in order to machine point sampled surface. In the adopted methodology, a guide surface having simpler geometry is created and the initial toolpath is planned on it based on the pattern which the cutter follows during the motion. For every point, the conforming CC point is positioned by projection process. In this, the point is projected on to the point cloud. To obtain CL points, a fitting approach is implemented. The approximation CC points using Bezier curve is performed. A method is also derived to position the points. This makes them evenly spaced along with equal arc lengths. To create toolpath using CMM was given by Lin et al. [4].To generate toolpath by using ball end mill from discrete points another approach was given by Feng et al. [**5**].In this method Cutter location data is generated which categorises them on the basis of permissible error and desired accuracy. Each CL data group is optimised and sequentially organised. This is done by minimising the error of each CL net shell. The extra CL points are then later trimmed in order to lower down the time taken to machine. For no gouge condition the size of ball end mill was governed. With the help of approximate normal vector the accuracy of the cutter size is determined. Teng et al. [12] presented an approach to generate efficient 3-axis NC toolpath using ball end mill directly from point cloud data. In order to attain the higher efficiency the entire machining surface is divided into different portions depending on how complex is the geometry, stool dimensions and patched portions. Kayal [20] suggested a methodology where the variables chosen were chordal error, scallop height and slope of curvature .The function of

above variables is developed to determine the machining error. Using Inverse offset method toolpath is generated by cloud of points. This leads to the generation of efficient and accurate toolpath by keeping the machining error in the desired range.

2.4 Toolpath Generation Based on STL Model

STL model generated from either point cloud [2] or from parametric model is very common in CAD/CAM systems [1,12]. The ease by which it can exchange data, perform geometric computation and become input to toolpath planning algorithms is the reason for its popularity with machinists for CAM applications [10]. This tessellated model increases the process of toolpath generation as only linear equations are required for the computation process [20]. The major advantage of using them is that they could be used even if they are somewhat defective or incomplete. An approach was presented for 3- axis to generate toolpath for sculptured surfaces [3]. The toolpath is gouge free and is generated from STL model. An offset for these models created and then sliced by driving planes. The curved segments are later fixed clipped and the concave gouge is omitted during the clipping phenomenon. Hence, convex and concave type gouging can be avoided in the generated cutter path. Iso-planar approach is very common with STL surfaces [2, 3, 8 and 22]. In this approach, design surface is cut by number of parallel planes to figure out the CC points. The CC points are used to calculate the CL points. These CL points are joined to create toolpath. Iso-parametric approach involves generation of toolpath that incurs surface data directly for toolpath generation. This approach provides better efficiency and accuracy with the generated toolpath. But, it produces non linearity in cartesian space for entities that are linear in parametric space [22]. Compensation is provided for the geometric errors. This leads to the increase in accuracy of the machined part. The cutter path is created from the original polyhedral model to machine a test part. The part is later scanned to form a 3D model which could later be utilised to generate toolpath [15]. Ren et al. [9] proposed a methodology to generate toolpath for pencil cut machining. In the approach, material side data is utilized for tracing phenomenon. This technique could be adopted in CAD/CAM schemes to obtain toolpaths to machine compound faceted model.

2.5 Tool Positioning Methods for 3- Axis Milling

To obtain tool location points it’s imperative to determine how the tool must be located at various positions along its trajectory. Hence, Tool positioning becomes an important step in the toolpath generation. Following approaches are used for tool positioning:

2.5.1 Surface offset method

Surface offset approach is adopted to find the cutter location surface which is intersected by the tool driving planes in order to generate tool driving curves [10]. To offset the surface is not an easy task and it causes self-intersection of the surface. Moreover, if the surface is freeform then the computation becomes more complex to obtain intersection curves. Also, with only ball end mill is most suitable with surface offset method because with other tool shapes the degree of complexity further increases. In the case of STL surface the problem of offsetting is though relatively simple which makes it popular among researchers. But, the computation is inefficient even though it's widely used.

2.5.2 Drop the tool method

For the ball nosed end milling cutter another robust method is given by Manos et al. [14]. In this approach the Z height is calculated by dropping the ball equal to the radius of the tool along the tool axis on each of the fixed tool positions in X-Y grid and the first contact point of the tool with the surface is recorded. Following are the steps to be followed to find the tool locations for STL model.

The method could also be used for the other tool shapes such as fillet end mill. But for fillet end mill, doughnut is dropped on the surface instead of a ball. This methodology of tool positioning is being adopted by other researchers also owing to its efficiency and robustness.

2.6 Tool Shape Effect on Surface Machining

The creation of the toolpath is essential for the machining of sculptured surfaces. For this, it requires suitable tool shape. To machine a flat part, flat end mills are mostly preferred as the profile of the tool exactly matches the surface. For the curved surface, ball end mill is preferred as it simplifies the task of toolpath creation. Gouge detection becomes easy with this tool shape. Radiused end mill enjoys the advantage of both flat and ball end mill. Present work employs ball end mill for the machining purpose as it's easy to position onto the desired surface and the calculation for the CL points becomes relatively simple and fast. Also, ball end mill provides greater surface finish when there is an abrupt change in the curvature [25].

2.7 Conclusion from Literature Review

From the various toolpath generation strategies studied in the literature survey, Cartesian offset toolpath planning algorithm has been most suited for the present work. Ball drop methodology suggested by Manos et al. [14] is implemented for positioning the tool since it provides gouge

free cutter location (CL) points for toolpath generation. STL model of the NURBS surface is preferred as an input to toolpath generation algorithm owing to the simplified calculation involved when compared to other data formats. Ball end mill is chosen for present work as it provides higher surface finish when machining a profile that contains abrupt change of slope. Also, it becomes easier to locate CL point in the case of Ball end mill. Algorithm to generate controlled scallop height by adjusting the side as suggested by Rajiv [26] is implemented.

Overall, present work focuses on the study of the effects of tool radius and iso-parametric discretization on the surface finish achievable by 3-axis vertical milling machine using ball end milling cutter. In this work, the mathematical model used for development of control scallop toolpath generation algorithm is presented along with the validation of the results from the developed algorithm for faceted freeform, concave and convex surfaces. Further this algorithm is used to identify the relationship between the tool dimensions, iso-parametric triangulation of NURBS surfaces and the surface finish that can be achieved within a reasonable number of machining passes.

Chapter 3 **Methodology**

In this work, a methodology for NC tool path generation for ball end milling cutter for a triangulated NURBS surface is presented. In this approach a generalized C++ program is developed for generation of iso-parametric point cloud for a NURBS surface developed though a user defined number of control points and user defined iso-parametric discretization. The developed C++ code is used to extract geometric information of the developed NURBS surface in the form of a uniform grid of iso-parametrically located points in the Cartesian space, henceforth referred to as NURBS point cloud data. The developed code also generates the triangulated model in the form of an STL file format to be used further for gouge-free toolpath generation for machining on a 3-axis vertical milling machine with a ball end milling cutter.

The toolpath generation algorithm used for toolpath computation for ball end milling cutter uses the concept of "*drop the tool*" and "*ray tracing algorithm*" in a unique way which ensures that the user defined scallop height is achieved by computing the adaptive side-step values for various machining passes for a zig-zag toolpath pattern with a uniform feed forward spacing of tool motion. The detailed methodology used in the present thesis work is described in detail in the following sections.

3.1 Selection of Parameters for Study

The parameters selected for the study in this dissertation work are listed in the Table 3.1.

Table 3.1 Parameter table

Type of surface	Triangulated NURBS surface
Cutting	Ball end mill
Methodology used for the toolpath generation	Drop the tool method [14]
Methodology used for validation of toolpath planning results	Use of NC simulator ToolSim [23] and Ray tracing algorithm [26]

3.1.1 3-D Data representation scheme for surface geometry

In present work, triangulated data as STL format is considered for the toolpath generation. It is the neutral format for the data exchange. In this format the 3D modelled surface is approximated by the set of triangles that are identified by three vertices and facet normal. There

are two types of data format for storing the information of the facet data: text (ASCII) format and Binary format. The major benefit of using STL file is that it has linear order equation that requires simpler calculations for tool path calculations. Hence, in the present work triangulation is done by generating STL file of ASCII data format from cloud of points that are grouped in an array in XY plane.

3.1.2 Adopted cutter shape and toolpath pattern

In present work, owing to the simplified calculation involved for toolpath creation and the ease at which it can be positioned on the desired surface, ball end mill cutter is chosen for the machining using Toolsim NC simulator. Also, it provides better surface finish when there is abrupt change in the curvature of the part to be machined.

Zigzag toolpath footprint pattern with cartesian toolpath planning approach is used for generating toolpath using ball nosed end milling cutter. Though machining with this footprint pattern takes more time when compared to other but it provides better constant cutting load [22]. The zig-zag toolpath footprint pattern is shown in Fig. 2.1 of the previous chapter.

3.1.1 Methodology for toolpath generation from triangulated model

Toolpath planning is a key aspect for getting desired output while machining of sculptured surfaces. Ball end mill is widely preferred by Industries for the machining of complex freeform surfaces [25]. For current work in order to determine cutter location points, ‘drop the tool’ method proposed by Manos et al. [14] is implemented. A sphere or a ball equal to the radius of ball end mill cutter is dropped alongside the axis of the tool, the first contact point with the surface is recorded and that point is the gouge free cutter location point (CL). To position the tool at this specific tool location the tool centre height is calculated based on the first contact point. Hence, the process of dropping the ball is continuously executed at regular time interval in order to obtain the tool height for each tool location. For Polyhedral models, ball end mill cutter could contact the surface in 3 probable scenarios as shown in Fig. 3.1. Tool can touch the face of any of the triangular facets of surface, it can touch any edge shared by two triangles or it may touch any vertex shared by two or more triangles. The complete equations to find the CL point is mentioned below for the triangle, edge and vertex check.

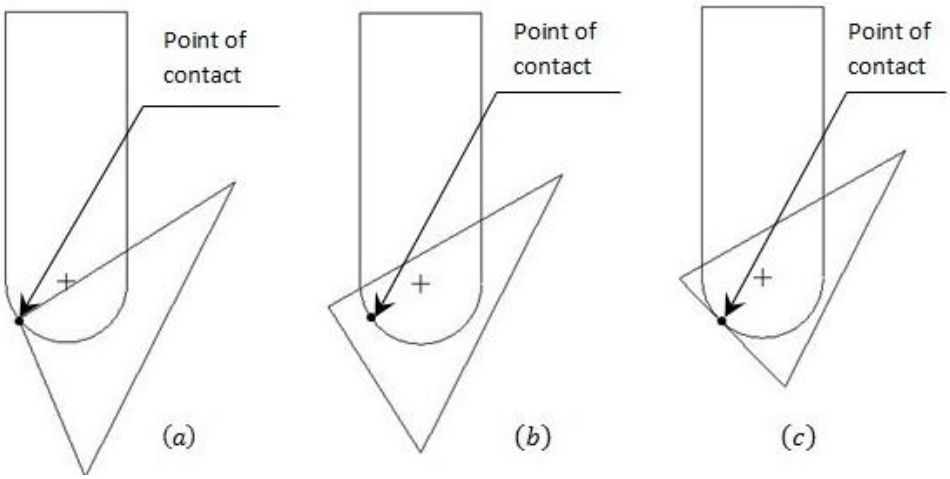

Figure 3.1: First contact with STL surface (a) vertex (b) face and (c) edge

In this method, the triangle check is performed to verify if the dropped ball touches the considered cylinder or not. Consider a tool radius r governed by the equation:

$$T(u) = T_1 + u(T_2 - T_1) \tag{3.1}$$

where, u is a parameter that specifies point between two extreme ends of the tool axis, T_1 and T_2. If the tool touches the face of the triangle bound by the vertices P_1, P_2 andP_3, it touches the face tangentially, since the tool's centre lies along tool axis. This gives rise to following equations:

$$T_1 + u(T_2 - T_1) = P_1 + (P_2 - P_1)t + (P_3 - P_1)s + \hat{N}r \tag{3.2}$$

Here s and t specify the point of contact between tool and the face of the triangle and

$$\hat{N} = \frac{(P_2 - P_1) \times (P_3 - P_1)}{|(P_2 - P_1) \times (P_3 - P_1)|}$$

If the triangle check gives no solution then the edge check is performed to check if the tool defined by equation 4.1 touches triangle's edge governed by equation:

$$P(u) = P_1 + u(P_2 - P_1) \tag{3.3}$$

If tool touches this edge, then following equation must be satisfied:

$$T_1 + u(T_2 - T_1) = P_1 + t(P_2 - P_1) + \hat{N}r \tag{3.4}$$

where,

$$\widehat{N} = \frac{(T_2 - T_1) \times (P_2 - P_1)}{|(T_2 - T_1) \times (P_2 - P_1)|}$$

This vertex check is implemented to see if tool touches any of three vertices of a triangle. The following equation must be satisfied if tool touches the vertexP_i:

$$|P_i - [(1-u)T_1 + uT_2]| = r \tag{3.5}$$

When the tool touches the vertex, there are two possible solutions. The solution which gives the highest tool center location which corresponds to largest value of u is taken as the final cutter location position for the given tool footprint location.

3.1.3 Methodology for validation of toolpath planning results

The validation for the toolpath is done in an open GL based graphical simulator ToolSim [23] and ray tracing algorithm is used to ensure that the user defined scallop height is achieved by computing the adaptive side-step values for various machining passes.

For validation, the NC toolpath data is generated for triangulated data which is as per the algorithm which is detailed in the subsequent sections. For comparison, the vertices are again extracted in a thick point cloud data and then corresponding to the spacing available, the ray traced space curved is used on the initial triangulated model of surface. Then error deviation between the two corresponding point for a given $x\ y$ location is found and then the deviation between the z heights are plotted and shown in the results chapter. This is how the validation of toolpath data is done.

3.2 Mathematical Model for NURBS Surface

The mathematical model for Non-uniform Rational B-Spline surface (NURBS) is used to produce triangulate data for a given set of data points is presented. It's a unified mathematical model which is a function of couple of parameters that maps in a 3D space. It is widely used in the representation of freeform curves and surfaces. The major advantage of using NURBS is that it allows the user to assign weights to each of the control point and thereby allowing user to control the behaviour of a geometric shape. The major advantage of using NURBS is that it provides enhanced manufacturing, speed and machining accuracy. Also, they are flexible and innate in nature for their use in design and geometric modelling. The formulation of NURBS is stated below:

A rational B spline surface P(u, v) having control points $n+1$ and $m+1$ in u and v direction is given by:

$$P(u,v) = \sum_{i=0}^{i=n} \sum_{j=0}^{j=m} \frac{\mathrm{P_{ij}h_{ij}}N_{ik\,(u)}N_{jl}(v)}{\mathrm{h_{ij}}N_{ik\,(u)}N_{jl}(v)} \tag{3.6}$$

Where,

$0 \le u \le u_{max}$ and $0 \le v \le v_{max}$.

$u_{max} = n - k + 2$ and $v_{max} = m - l + 2$.

$\mathrm{h_{ij}}$ is the weight associated with the control point P(u, v).

$k-1$ and $l-1$ denotes degree in $'u'$ and $'v'$ direction respectively.

If $\mathrm{h_{ij}}$ becomes unity, the rational B spline surface (NURBS) converts to Non-Rational B-spline. The values of basis function $N_{ik}(u)$, $N_{jl}(v)$ and knot vectors t_i and t_j are given as:

$$N_{ik}(u) = \frac{(u-t_i)N_{i,k-1}}{t_{i+k-1}-t_i} + \frac{(t_{i+k}-u)N_{i+1,k-1}}{t_{i+k}-t_{i+1}} \ ,$$

$$N_{jl}(v) = \frac{(v-t_j)N_{j,l-1}}{t_{j+l-1}-t_j} + \frac{(t_{j+l}-u)N_{j+1,l-1}}{t_{j+l}-t_{j+1}} \tag{3.7}$$

Where,

$$t_i = \begin{cases} 0 & ; i < l \\ i-k+1 & ; i \le j \le m \\ n-k+2 & ; i > m \end{cases}$$

$$t_j = \begin{cases} 0 & ; j < l \\ j-l+1 & ; l \le j \le m \\ m-l+2 & ; j > m \end{cases}$$

Where, $0 \le i \ge n+k$ and $0 \le j \le m+l$. The above relation illustrates that $n+k+1$ and $m+l+1$ is the length of the knot vector in $'u'$and $'v'$direction respectively.

Now, the triangulation of NURBS surface is done by generating STL file of ASCII data format from cloud of points that are grouped in an array in XY plane. Stitching algorithm has been implemented for the stitching of the points so as to produce triangles.

3.3 Toolpath Generation Algorithm

For the generation of toolpath iso-parametric and iso-planar techniques are most widely used. Uniform step in parametric space leads to toolpath with non-uniform step size. It is the major

cause of unequal scallops across the surface while iso-planar toolpath is more used for compound and trimmed surface. Hence, both the above methods lead to conservative toolpath when the attempt is made to control the scallop height. In present work, maximum scallop height is kept within the tolerance limit by using Bisection method and constant scallop toolpath is thus generated.

3.3.1 Computation for controlled scallop height

In the present work, scallop height is determined by using the methodology suggested by Rajiv [26]**.** In this method a ray is projected through the point M and I_C in order to calculate the scallop height. Point M defines the centre of the line joining the points C_{L11} and C_{L21} as shown in Fig. 3.2.The two cutter locations points are separated by distance of S_S value. Point I_C is generated by the point of intersection of two spheres. This represents the tool at two adjacent locations when projected on the plane which is normal to the feed forward direction and passing through points C_{L11} and C_{L21}. I_{stl} denotes the point where the ray strikes the surface. When the calculations are done along the direction of the ray projected, the distance between points I_C and I_{stl} provides the value of scallop height. The point I_C is governed as:

$$I_C = M + \hat{w}.r \tag{3.8}$$

Where, r denotes the radius of the circle of intersection between two spheres having the centres S_s distance apart which is shown in the Fig.3.2. Using the relation r= $\sqrt{(R^2 - l^2)}$, the value of radius is calculated and the value of l is given by the relation:

$$l=|(C_{L11} - M)| \tag{3.9}$$

The value of the unit vector $\hat{w}$ is determined using the following equations:

$$\hat{u} = \frac{M - C_{L11}}{|M - C_{L11}|} \tag{3.10}$$

$$\hat{v} = \frac{\hat{u} \times \hat{t_l}}{|\hat{u} \times \hat{t_l}|} \tag{3.11}$$

$$\hat{w} = \frac{\hat{u} \times \hat{v}}{|\hat{u} \times \hat{v}|} \tag{3.12}$$

where,

$$\hat{t} = \{0,0,1\}$$

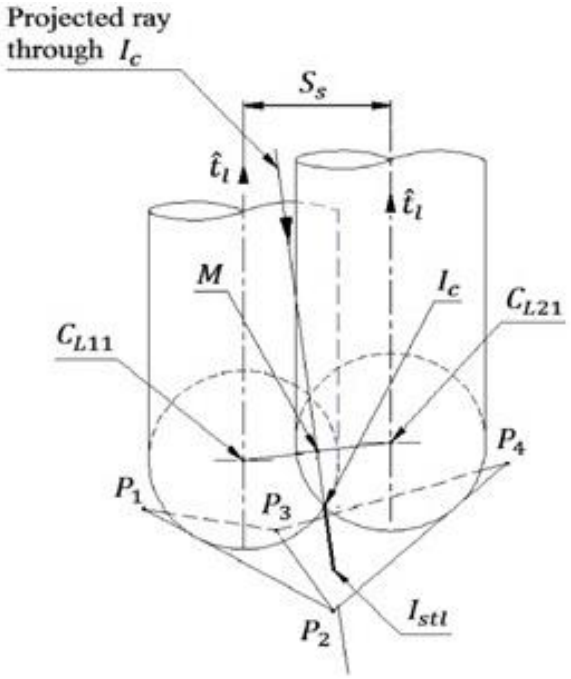

Figure 3.2: Scallop height calculation [26]

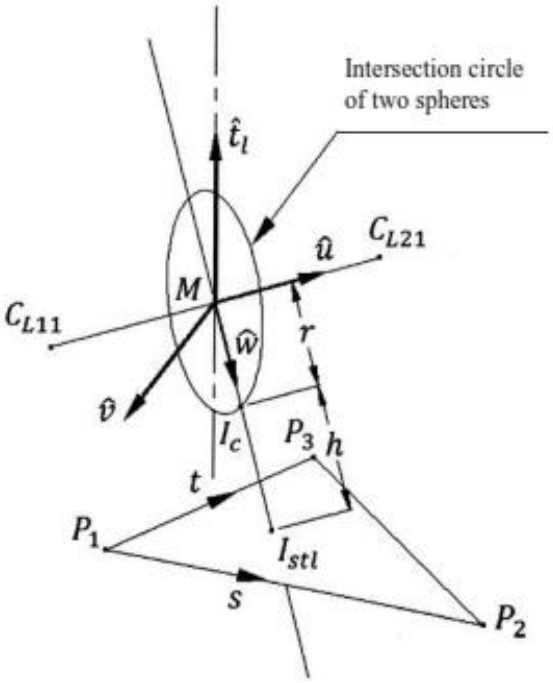

Figure 3.3: Intersection circle of two spheres [26]

The scallop height h can be easily noticed from the Fig. 3.3. To determine the value of h, I_{stl} is to be known first. It is the point at which the ray from I_c intersects with the triangle $P_1P_2P_3$ along the unit vector $\hat{w}$. I_{stl} can be expressed in parametric domain as:

$$I_{stl} = P_1 + s(P_2 - P_1) + t(P_3 - P_1) \tag{3.8}$$

Where,

$$0 \leq (s, t, s + t) \leq 1$$

also,

$$I_c + h\hat{w} = I_{stl} \tag{3.9}$$

Concluding from equations (3.1) and (3.2):

$$I_c + h\hat{w} = P_1 + s(P_2 - P_1) + t(P_3 - P_1) \tag{3.10}$$

$$\Rightarrow h\hat{w} + s(P_1 - P_2) + t(P_1 - P_3) = P_1 - I_c$$

or
$$h\hat{w} + sA + tB = C \tag{3.11}$$

where,

$$A = (P_1 - P_2), B = (P_1 - P_3), C = (P_1 - I_c)$$

The above equation can be written in matrix form as:

$$\begin{bmatrix} \hat{w}_x & A_x & B_x \\ \hat{w}_y & A_y & B_y \\ \hat{w}_z & A_z & B_z \end{bmatrix} \begin{bmatrix} h \\ s \\ t \end{bmatrix} = \begin{bmatrix} C_x \\ C_y \\ C_z \end{bmatrix} \tag{3.12}$$

or
$$\begin{bmatrix} h \\ s \\ t \end{bmatrix} = \begin{bmatrix} \hat{w}_x & A_x & B_x \\ \hat{w}_y & A_y & B_y \\ \hat{w}_z & A_z & B_z \end{bmatrix}^{-1} \begin{bmatrix} C_x \\ C_y \\ C_z \end{bmatrix} \tag{3.13}$$

The values of s and t must satisfy the below condition

$$0 \leq (s, t, s + t) \leq 1$$

If the above mentioned condition is satisfied the value of h is taken to be as a solution. Similarly the value of 'h' is calculated for each triangle intersecting with the ray. The largest value of h signifies maximum scallop height.

3.3.2 Side step adjustment

In order to achieve the scallop height value ε (user defined), side steps are optimized by bisection method used by Rajiv [26]. Initial side step value S_{si} is chosen and iteration between

the limits S_{sl} and S_{sr} is performed to achieve scallop height value same as to ε as shown in Fig. 3.4. In present work, first the reference toolpath is generated having the constant value of feed forward steps. These steps serve as the side steps for the next derived toolpath. This derived toolpath contains the same feed forward step values as that of reference toolpath with the adjusted value of side step in order to control the scallop height. The minimum side step value is chosen and recorded to generate the straight toolpath line parallel to the reference line. This toolpath would serve as the reference toolpath for the next line and the process continues until the final toolpath line is achieved. In this way, toolpath with adjusted side step value and constant feed forward value is achieved which is shown in the Fig. 3.5.

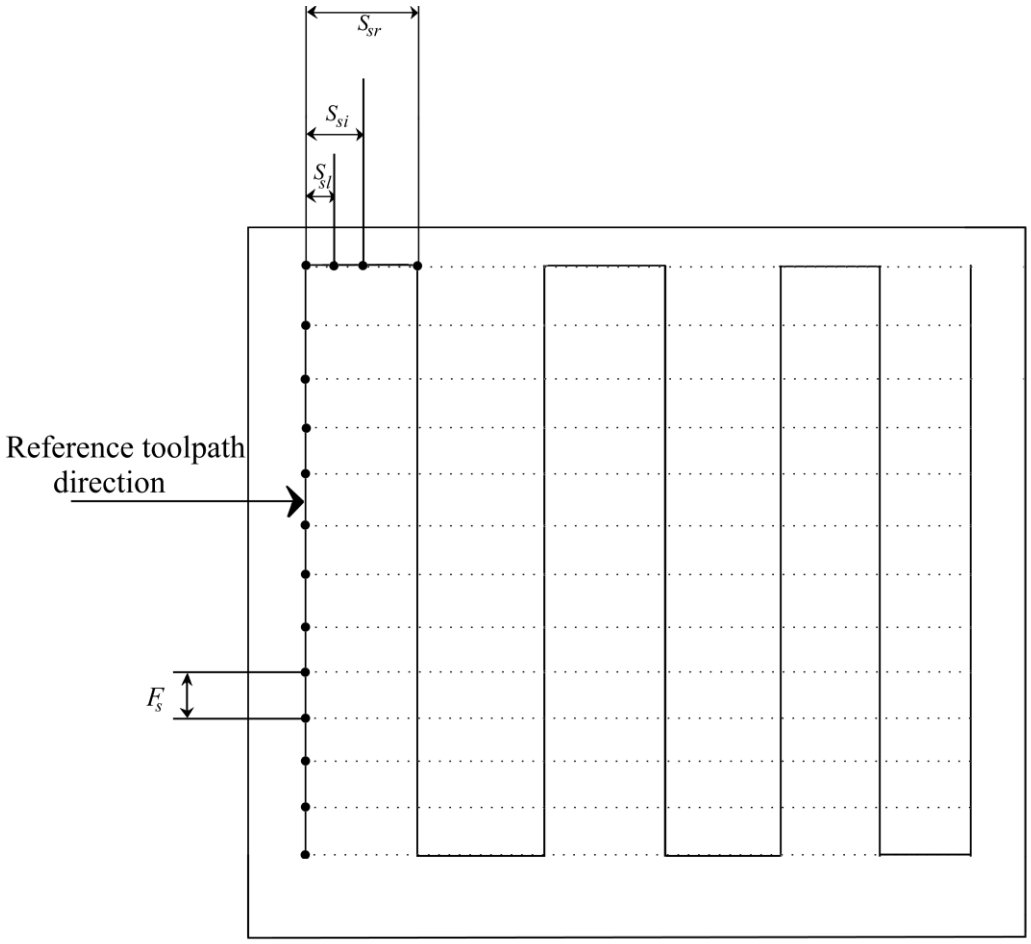

Figure 3.4: Side step adjustment using bisection method [26**]**

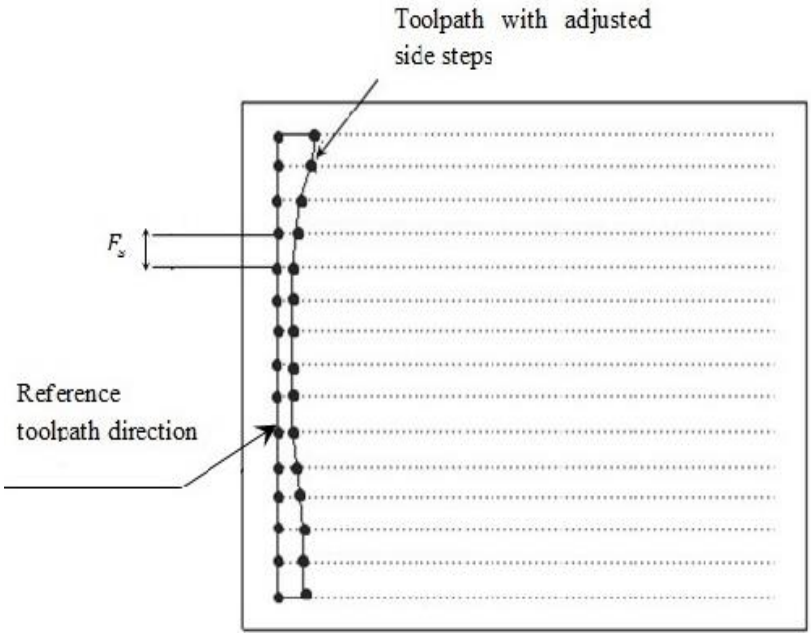

Figure 3.5: Side step adjustment for constant scallop height [26]

3.4 Solution Scheme

The overall methodology used in the present dissertation work has been presented in the flowchart represented in Fig.3.6 and the summary of the procedure used in the solution scheme is given below:

1. Initially the input is given in the form of control points and degree of NURBS surface, iso-parametric spacing for generation of point cloud data for triangulation of NURBS surface, tool radius, scallop height required, feed forward and initial side step values for zig-zag toolpath.
2. Generation of iso-parametric point cloud data for NURBS surface
3. Generation of triangulated facets and storage of triangulated NURBS surface data in STL format.
4. Use of "*drop the tool*" algorithm to generate initial reference toolpath and use of "*constant scallop height*" algorithm to generate toolpath data for specified radius of ball end mill.

The detailed results obtained from the methodology presented in this chapter is presented and discussed in the next chapter.

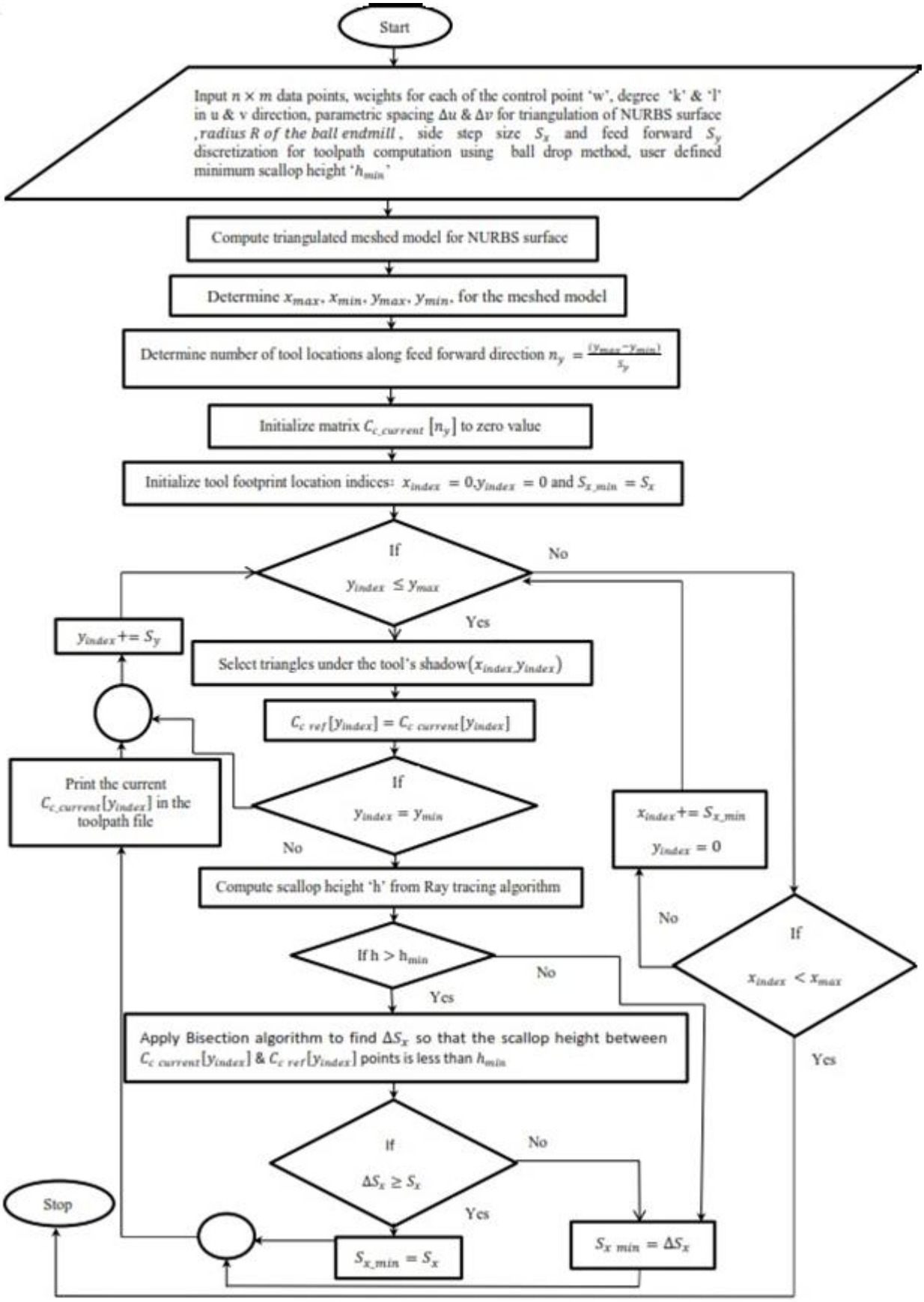

Figure 3.6: Overall flowchart for toolpath

Chapter 4 Results and Discussions

In this chapter, the results obtained for constant scallop height toolpaths generated for ball end milling cutter, for triangulated NURBS surface is presented. The flowchart and overall solution scheme used is presented in section 3.5 of the previous chapter. Three types of NURBS surface with 5×5 number of control points are taken for the study purpose. The details of the selected NURBS surface as well as other parameters along with the results generated for various cases are systematically presented below.

4.1 Input Parameters used for the Present Study

The input parameters taken for the present study are shown in Table 4.1.

Table 4.1: Input parameters

Model type	NURBS surface models
Iso-parametric discretization level	0.001, 0.025,0.050,0.075 and 0.10
Shape of surfaces	Freeform, concave and convex
Radius of ball end mill(r)	1.5875mm, 3.175mm and 6.35 mm
Feed forward distance (F_s)	1 mm
Initial side step value(S_{si})	1 mm

4.2 Details of surface models used for the present study

As represented in the input parameter table, the three shapes of surface model that are studied for the toolpath generation are:

- Freeform surface
- Concave surface
- Convex surface

The coordinate values for freeform NURBS surface is represented in Table 4.1, for concave NURBS surface is represented in table y and for convex NURBS surface is represented in table z and corresponding triangulated images are shown in Fig. 4.1. The triangulated images are captured from STL viewer "DeskArtes 3Data Expert 8.1" (freeware). The corresponding triangulated surface model at various levels of discretization for freeform, concave and convex NURBS surface is shown in Fig. 4.2-4.4.

Table 4.2-4.3 shows the coordinates of control point for the different NURBS shapes taken for the study. The value of the weight h assigned to each of the control point is taken as unity.

Table 4.2: Coordinates of freeform NURBS test surface

$P_{i,j}$	0	1	2	3	4
0	(0.0,0.0,15.0,)	(12.5,0.0,17.5)	(37.5,0.0,17.5)	(37.0,0.0 ,25.0)	(50.0,0.0,15.0)
1	(0.0,12.5,17.5)	(12.5,12.5,20.0)	(25.0,12.5,22.5)	(37.5,12.5,20.0)	(50.0,12.5,17.5)
2	(0.0,25.0,20.0)	(12.5,25.0,22.5)	(25.0,25.0,25.0)	(37.5,25.0,22.5)	(50.0,25.0,20.0)
3	(0.0,50.0,15.0)	(12.5,37.5,20.0)	(25.0,37.5,22.5)	(37.5,37.5,20.0)	(50.0,37.5,17.5)
4	(0.0,50.0,15.0)	(12.5,50.0,17.5)	(25.0,50.0,20.0)	(37.5,50.0,17.5)	(50.0,50.0,15.0)

Table 4.3: Coordinates of concave NURBS test surface

$P_{i,j}$	0	1	2	3	4
0	(0.0, 0.0, 25.0)	(12.5,0.0,22.5)	(25.0,0.0 ,20.0)	(37.0, 0.0 ,25.0)	(50.0,0.0,25.0)
1	(0.0,12.5,22.5)	(12.5,12.5,20.0)	(25.0,12.5,17.5)	(37.5,12.5,20.0)	(50.0,12.5,22.5)
2	(0.0,25.0,20.0)	(12.5,25.0,17.5)	(25.0,25.0,15.0)	(37.5,25.0,17.5)	(50.0,25.0,20.0)
3	(0.0,37.5,22.5)	(12.5,37.5,20.0)	(25.0,37.5,17.5)	(37.5,37.5,20.0)	(50.0,37.5,22.5)
4	(0.0,50.0,25.0)	(12.5,50.0,22.5)	(25.0,50.0,20.0)	(37.5,50.0,22.5)	(50.0,50.0,25.0)

Table 4.4: Coordinates of convex NURBS test surface

$P_{i,j}$	0	1	2	3	4
0	(0.0,0.0,15.0)	(12.5,0.0,17.5)	(37.5,0.0,17.5)	(37.0,0.0,25.0)	(50.0,0.0,15.0)
1	(0.0,12.5,17.5)	(12.5,12.5,20.0)	(25.0,12.5,22.5)	(37.5,12.5,20.0)	(50.0,12.5,17.5)
2	(0.0,25.0,20.0)	(12.5,25.0,22.5)	(25.0,25.0,25.0)	(37.5,25.0,22.5)	(50.0,25.0,20.0)
3	(0.0,37.5,17.5)	(12.5,37.5,20.0)	(25.0,37.5,22.5)	(37.5,37.5,20.0)	(50.0,37.5,17.5)
4	(0.0,50.0,15.0)	(12.5,50.0,17.5)	(25.0,50.0,20.0)	(37.5,50.0,17.5)	(50.0,50.0,15.0)

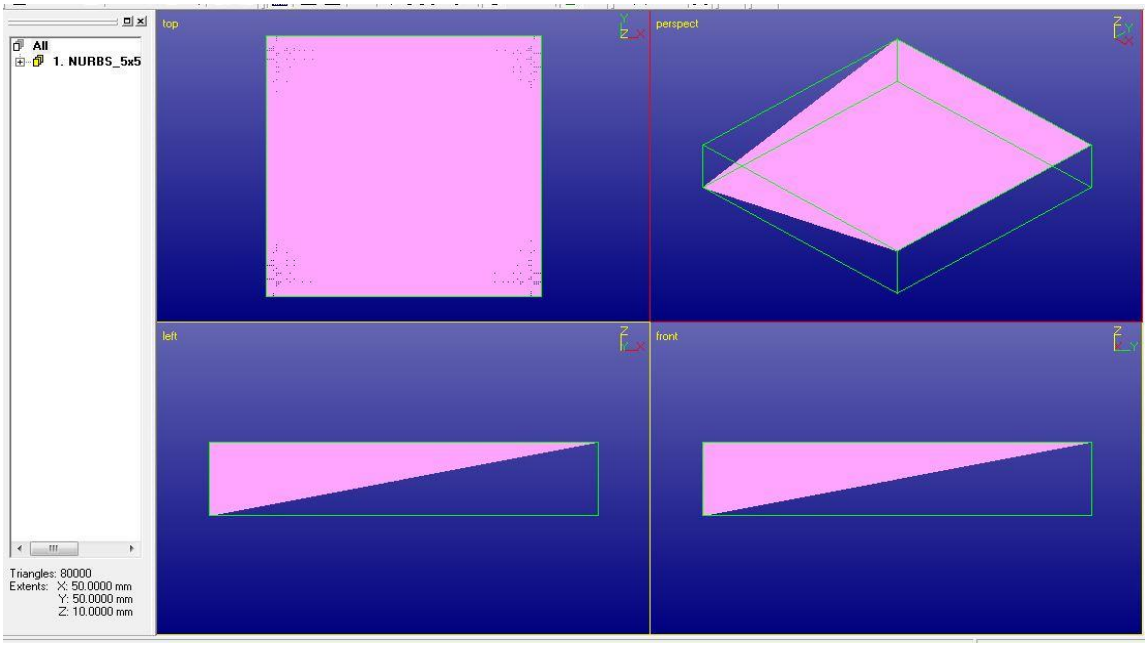

(a)

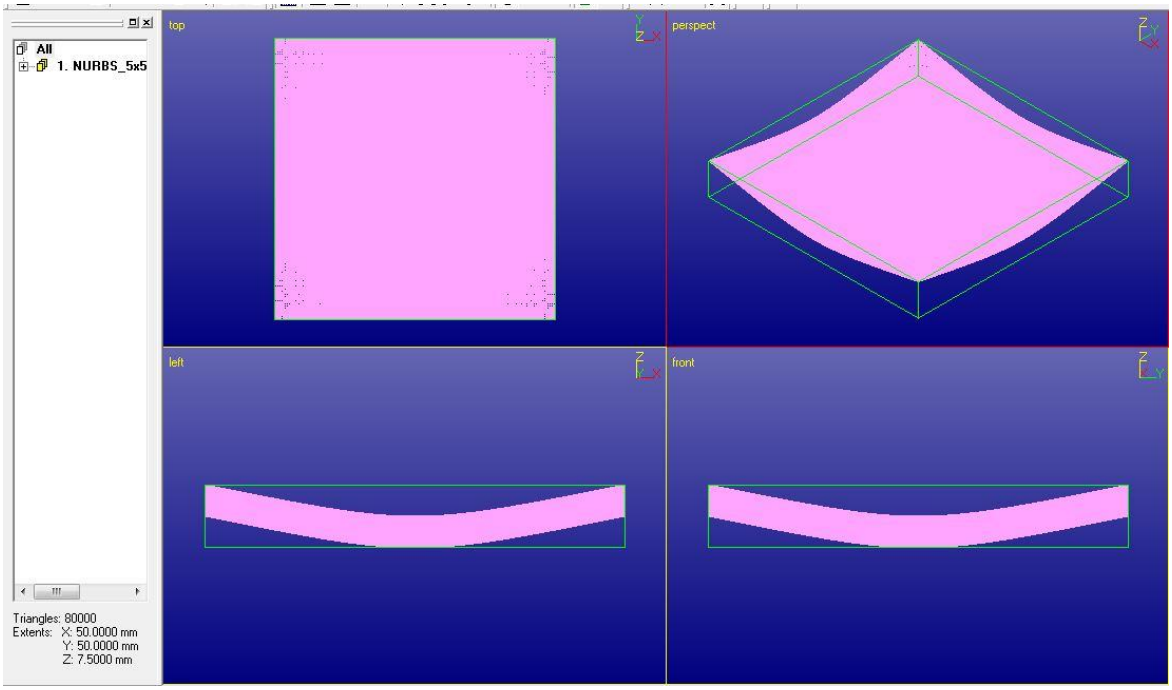

(b)

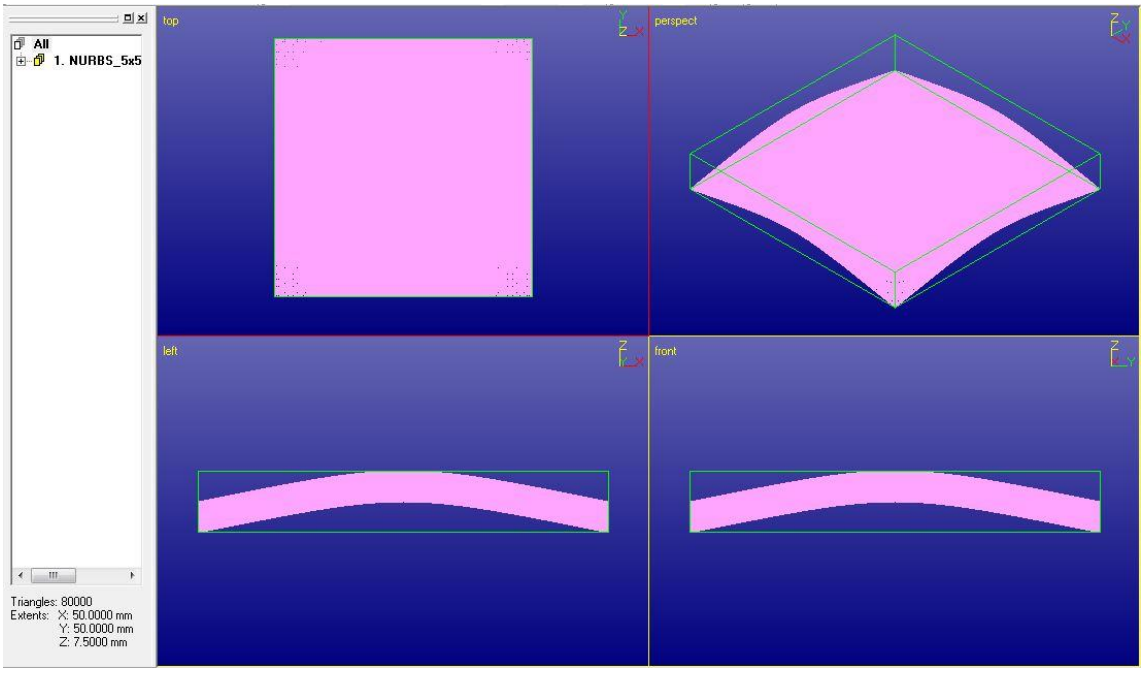

(c)

Figure 4.1: (a) Freeform NURBS, (b) concave NURBS and (c) convex NURBS surface test part

The iso-parametric discretization level $UV = 0.01$ is chosen for the verification of the machining results. This discretization level is precise and it approximately reflects the points corresponding to the actual NURBS surface. The point cloud data obtained from this

discretization level is used for the generation of points on the curve on the surface which is used later for the comparison of machining simulation results obtained from ToolSim 3-Axis NC simulator available in SIDC laboratory at Thapar University, Patiala.

The NURBS surface parts analysed for the study purpose and are discretized iso-parametrically for four different levels of UV to create triangulated surface model. The values of UV used for the study in the present work are 0.025, 0.05, 0.075 and 0.10 with the tool radius mentioned in the input parameters shown in Table 4.1.

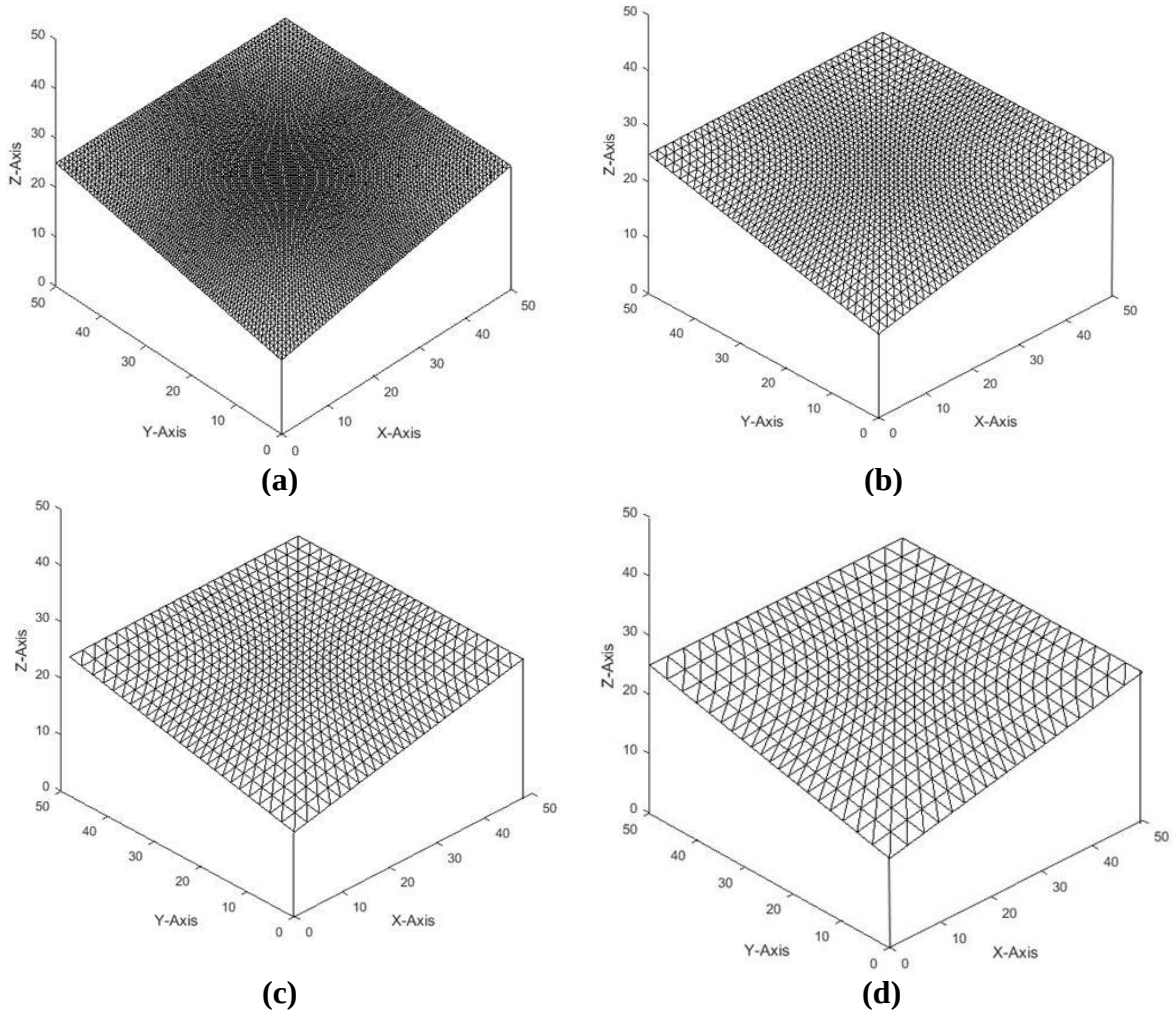

Figure 4.2: Freeform triangulated NURBS surface with iso-parametric discretization level of (a) 0.025, (b) 0.050, (c) 0.075 and (d) 0.10

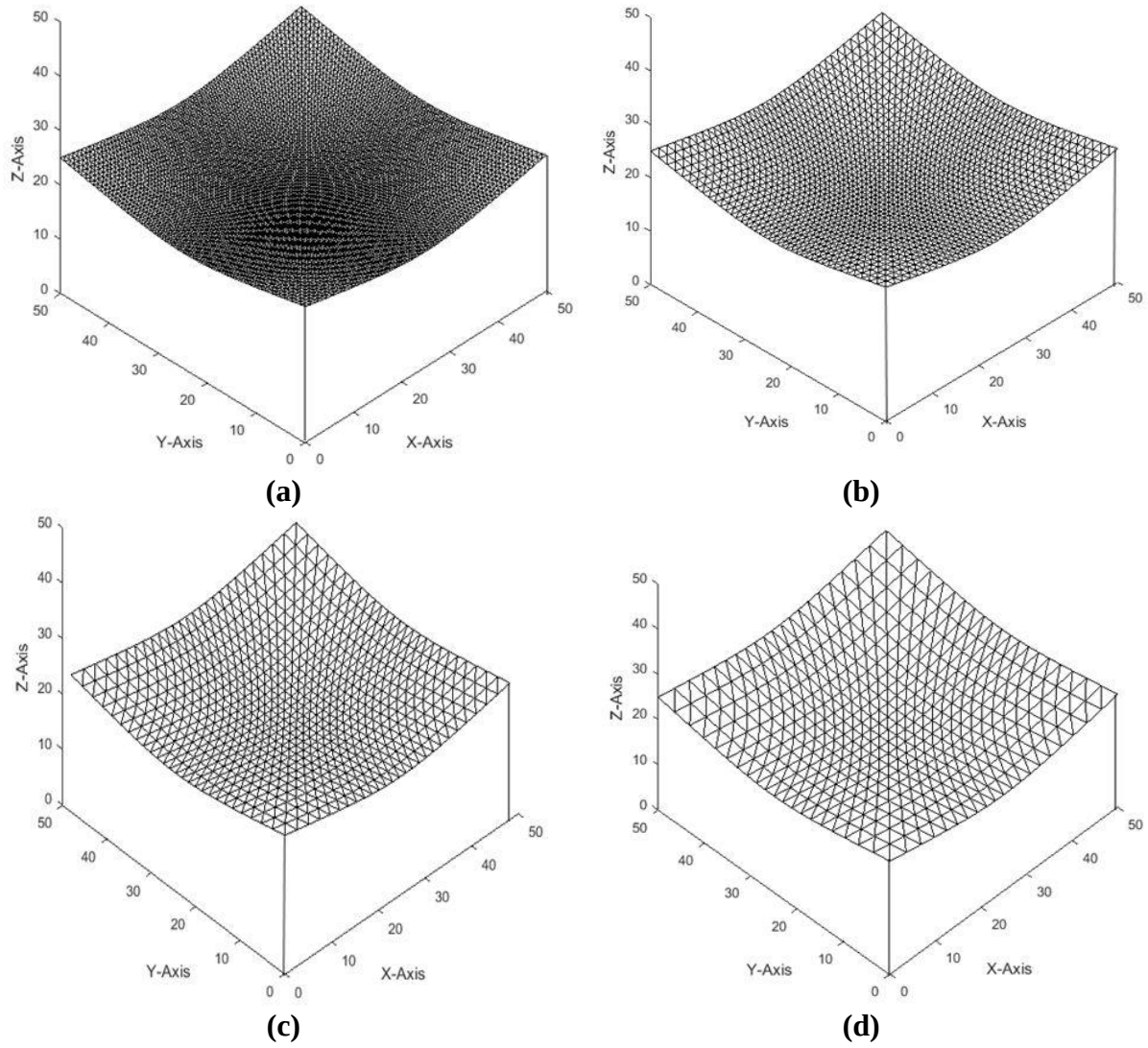

Figure 4.3: Concave triangulated NURBS surface with iso-parametric discretization level of (a) 0.025, (b) 0.050, (c) 0.075 and (d) 0.10.

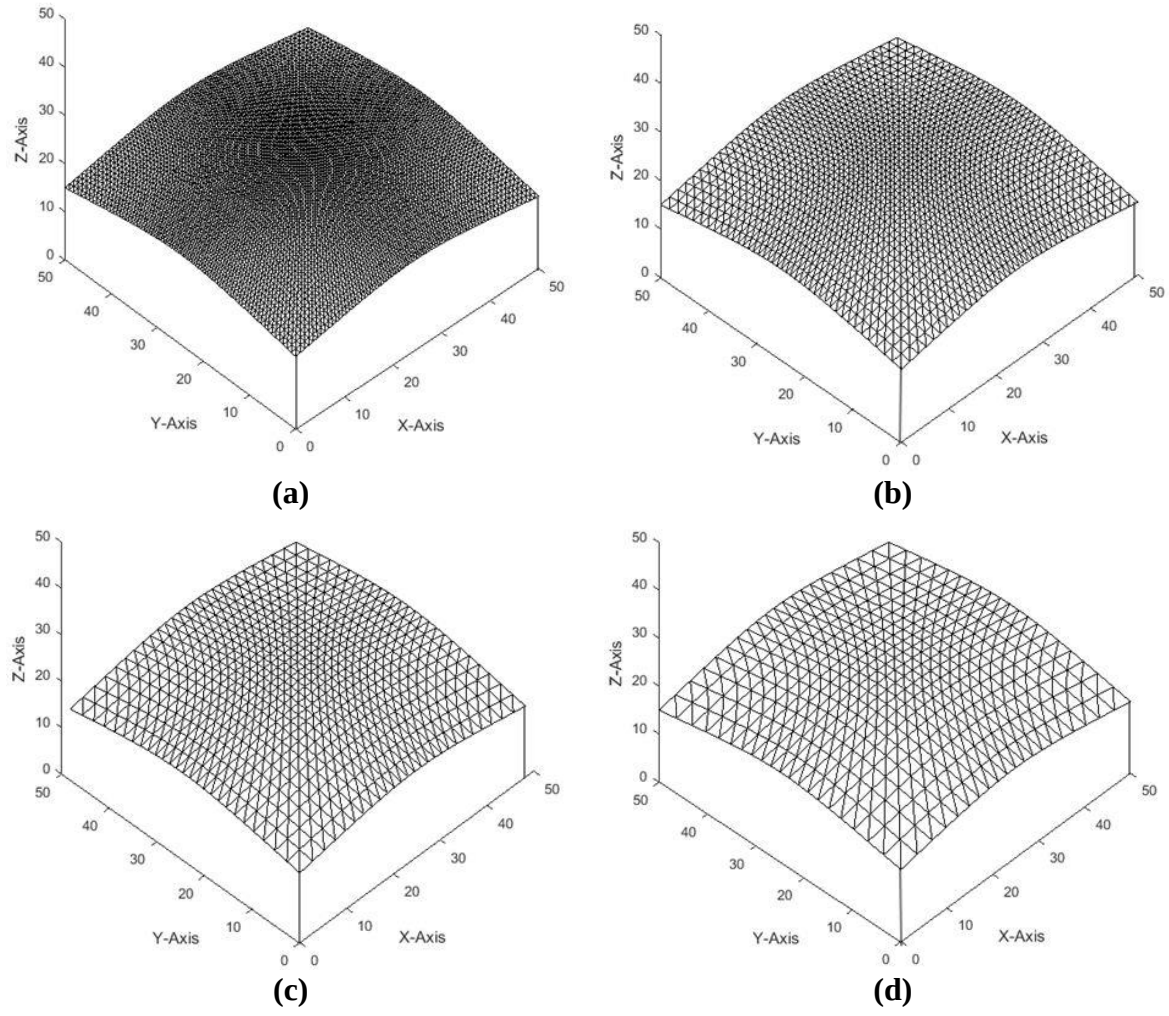

Figure 4.4: Convex triangulated NURBS surface with iso-parametric discretization level of (a) 0.025, (b) 0.050, (c) 0.075 and (d) 0.10

4.3 Validation

The four levels of iso-parametric discretization for each of the three NURBS surface model are studied to establish the relationship between the tool radiuses, facet size of triangulated surface and surface finish achievable within the reasonable number of machining path. Therefore, by using the toolpath generation algorithm, toolpaths for three triangulated NURBS surface model at four different discretization level are generated to figure out the minimum value of user defined scallop at which reasonable number of machining passes are obtained, by using each of the three size of ball end milling cutter for every NURBS shape. The result shows that reasonable number of tool passes were achieved within the scallop height of 35 microns in case of tool of radius 1.5875 mm, scallop height of 65 microns in the case of 3.175 mm tool radius and scallop height of 130 microns with the tool radius of 6.35mm.Though, the exceptions were seen with freeform surface with discretization level of 0.025 and 0.075 when tool of radius

6.35 mm radius was used. The detailed results for the minimum value of scallop height achieved by the tool with each of the NURBS shape for given value of ε is shown in the Table 4.5.

But, if the value of user defined scallop height further is reduced by 5 microns, redundant toolpaths are obtained for all the 3 shapes with tool radius of 1.5875 mm and discretization level $UV = 0.025$.

Figures 4.5(a)-4.7(a) shows that the redundant toolpaths are observed with $\varepsilon = 0.030mm$ and tool passes with reasonable value of side step intervals for the next two consecutive value of ε with an increment of $\Delta 0.005$. The similar cases are shown for concave NURBS and convex NURBS surface. The tool passes for the $\varepsilon = 0.035\text{mm}$ and $\varepsilon = 0.040\text{mm}$ for each NURBS shape shown below in Fig. 4.5-4.7 and the toolpath interval is reasonable and it's neither too less nor too large which shows that the constant scallop toolpath generation algorithm is able to manage the user specified scallop height constraint within stipulated tolerance limit .

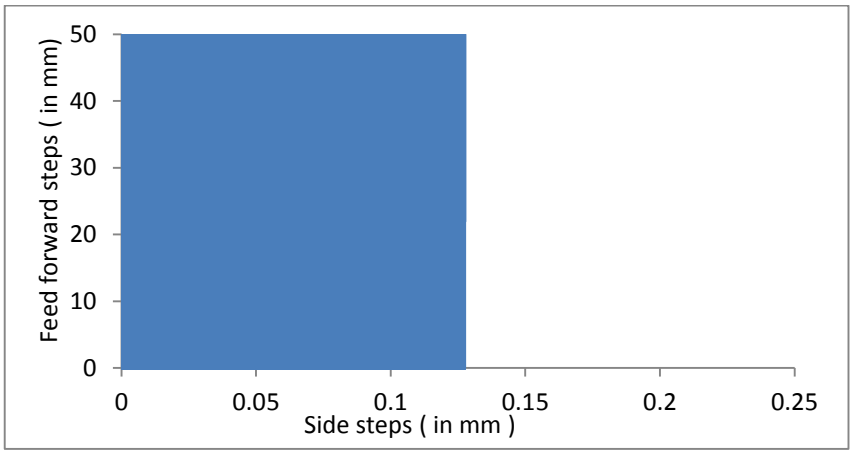

(a)

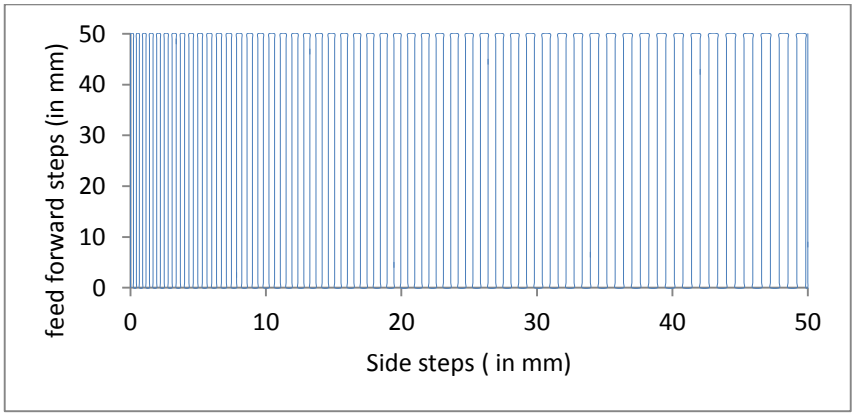

(b)

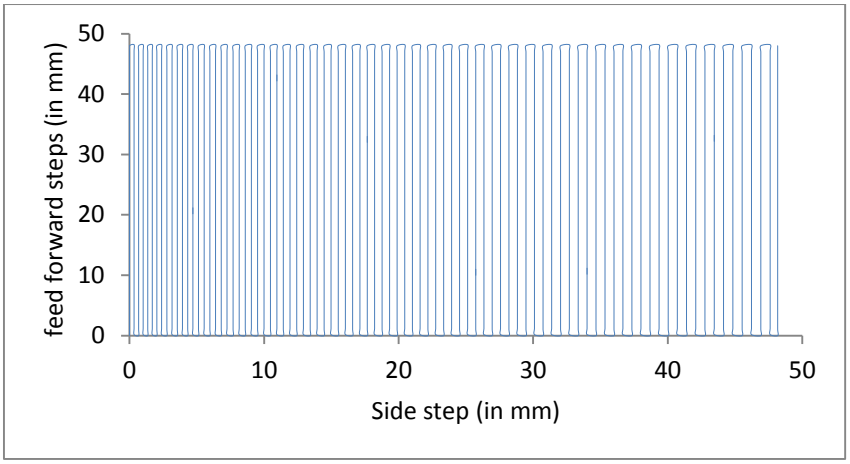

(c)

Figure 4.5: Tool passes for Freeform NURBS surface with (a) $\varepsilon = 0.030$ (b) $\varepsilon = 0.035$ c) $\varepsilon = 0.040$

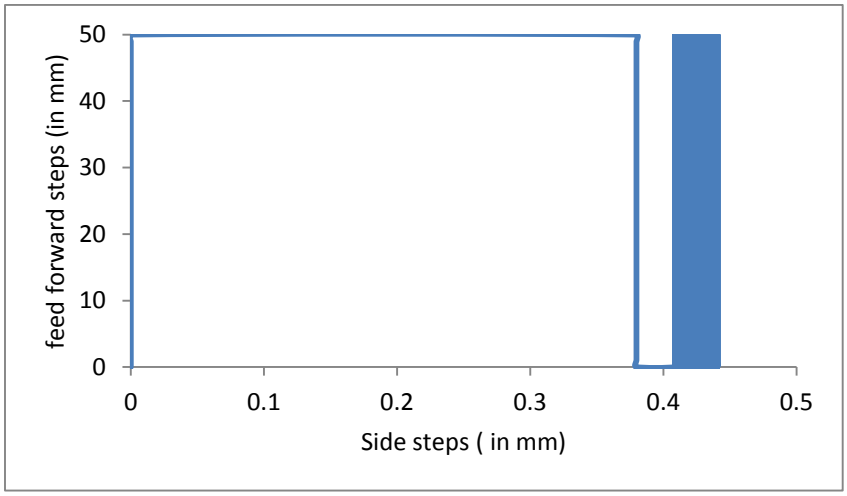

(a)

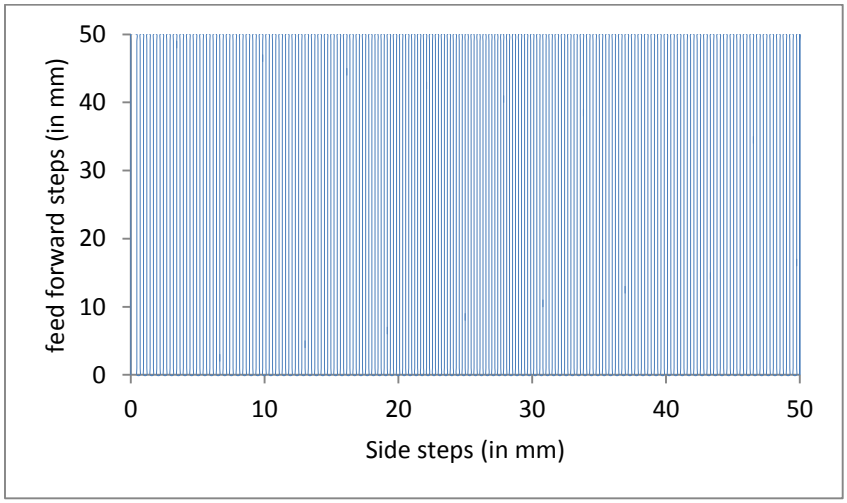

(b)

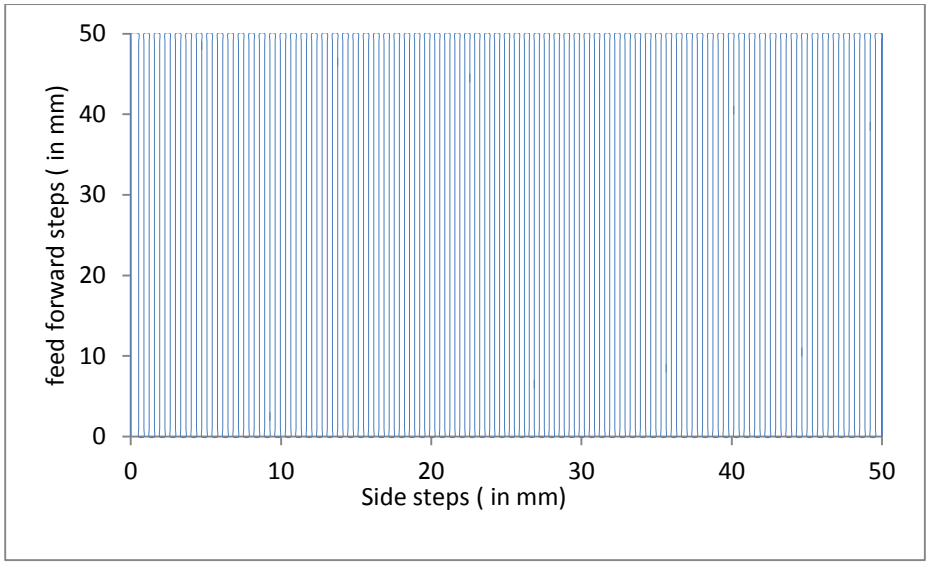

(**c**)

Figure 4.6: Tool passes for concave NURBS surface (a) $\varepsilon = 0.030$ (b) $\varepsilon = 0.035$ c) $\varepsilon = 0.040$

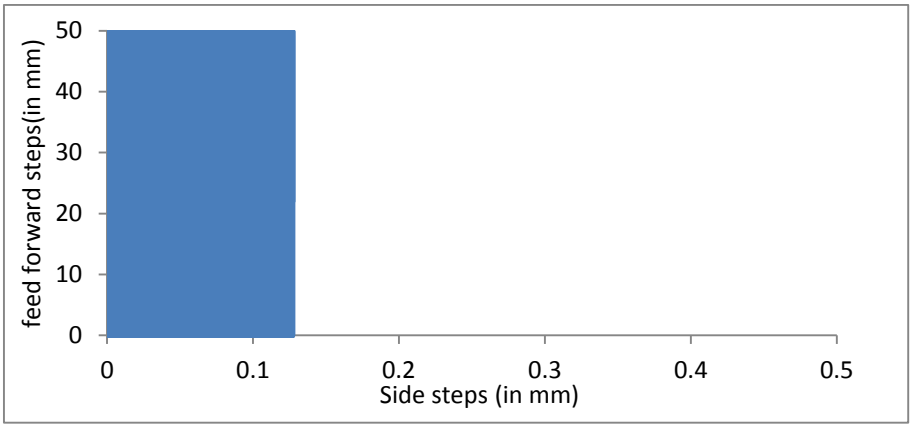

(a)

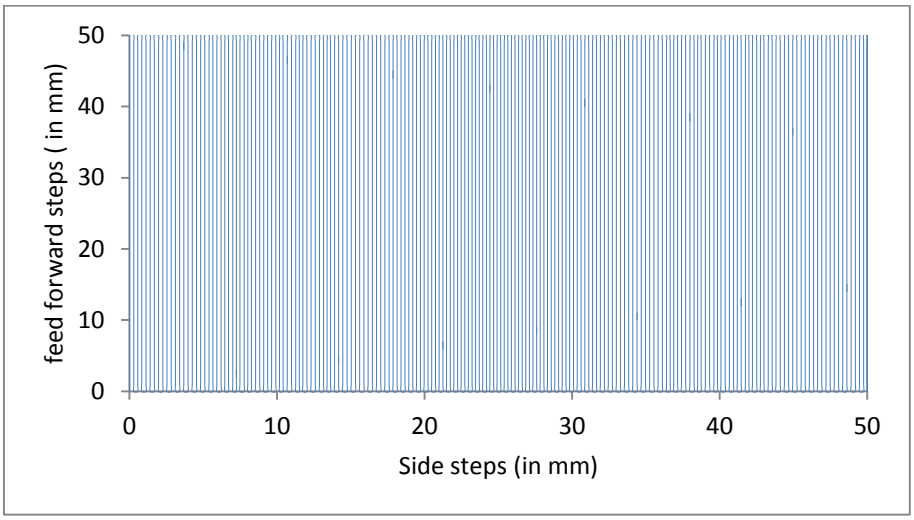

(b)

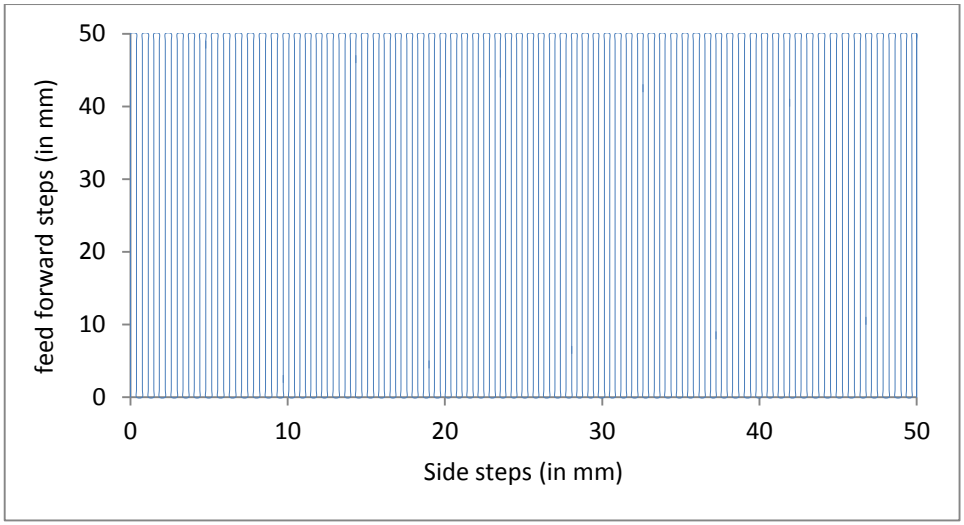

(c)

Figure 4.7: Tool passes for convex NURBS surface (a) $\varepsilon = 0.030$, (b) $\varepsilon = 0.035$ and (c) $\varepsilon = 0.040$

The validations of the above results are done by comparing simulation stock from ToolSim graphical simulator where the created toolpath were used to generate simulated machined surface. The shape of the machined surface in 3-axis NC simulator is captured as a 3D point cloud data which is saved in object file from open GL environment of simulator. The density of the point cloud can be varied for generating machining simulated data. The value of density is taken in present work as 50×50 per square inch and 508×508 per square inch. The former value of density is used to establish a relational deviation between the curves obtained under NURBS surface found from iso- parametric discretization of triangulated data at a level $UV = 0.01$ while the latter value of density is used to validate the results of constant scallop height toolpath algorithm. The work of this algorithm is shown for the freeform, concave and convex NURBS test surface. The radius of the ball end mill cutter for machining simulation is taken as 1.5875 mm.

Figure 4.8 below shows the comparison between the scallops obtained from object file data and points after ray tracing of NURBS triangulated surface for each of the three shapes with discretization level of 0.025.The surface error lies within the range of 30 microns for freeform surface shown in Fig. 4.8(a) and for concave and convex NURBS surfaces the scallop height at the entry and exit of tool lies beyond the specified tolerance limit but for the middle region of the surface height of the scallops encountered are in the range of 30 microns as shown in Fig. 4.8(a) and 4.8(b). The graph shown in Fig. 4.8 shows that the error scallop height is under control and lies within the range of 30 microns for all the three shapes of NURBS surface.

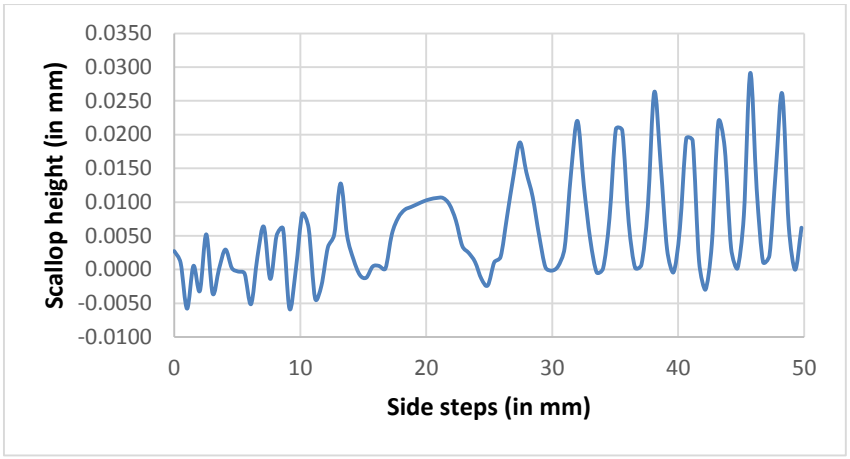

(a)

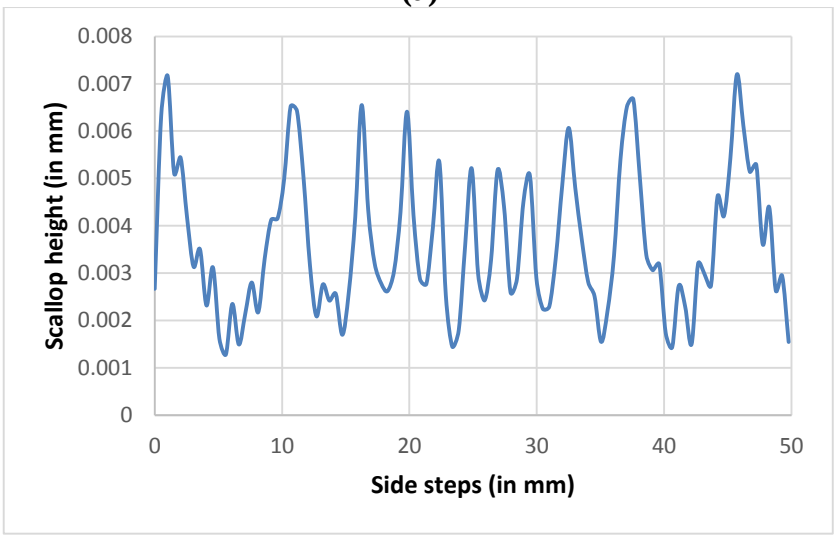

(b)

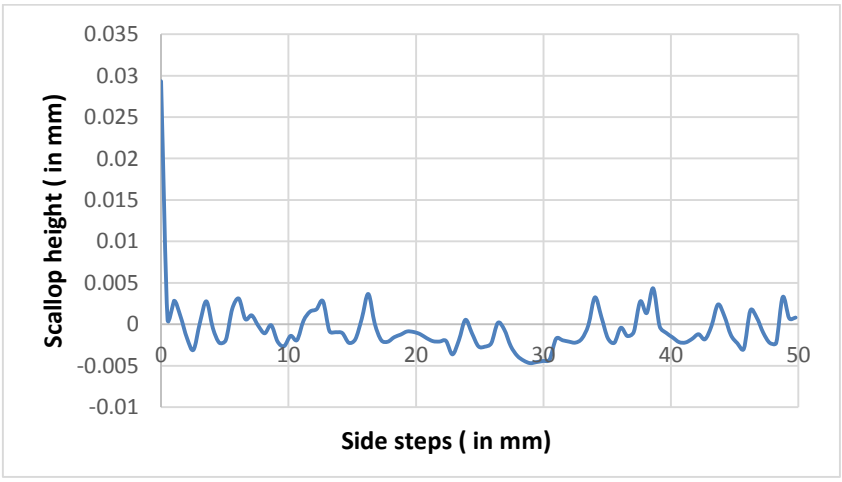

(c)

Figure 4.8: Comparison of the scallops for (a) freeform NURBS surfaces, (b) concave NURBS surface and (c) convex NURBS surface

The graphical comparison between surface finish obtained in graph is done. Simulations for three part freeform, concave and convex part with minimum iso-parametric discretization level $UV = 0.025$ is done. Therefore, the point cloud data from graphical simulator was obtained for machining these parts by tool radius of 1.5875 mm.

4.4 Comparison of Results

The projected curve shape of the three NURBS surface parts was obtained by ray tracing of 0.01 iso-parametric discretization of triangulated NURBS surface (for each of the three types) which is used as reference. With this curve called reference surface curve comparison of the data obtained from graphical simulator for middle most region of the three NURBS surfaces test parts at y $= 25$ mm and at $y = 15\ mm$ is performed .The range of points from $x = 0$ to $x = 50$ is obtained from graphical simulator as well as on reference curve using ray tracing. This comparison for the three NURBS shapes is discussed below in subsequent sections.

4.4.1 Freeform NURBS surface

Figure 4.9 are the plots for the differences in error for surface profile curve generated by using ray tracing on NURBS surface (triangulated with discretization level of 0.01) and STL surface with discretization level $UV = 0.0250$ taken with respect to the object surface generated from ToolSim graphical simulator.

Figure 4.10 shows the comparison of the data obtained from graphical simulator in the case of freeform NURBS surface for $y = 25\ mm$ .The graph depicts that the data lies within the range of 30 microns though at some areas, greater scallop height is achieved but for the middle portion i.e. for $x = 24.5\ mm\ to\ x = 25.5\ mm$, scallop height is within the permissible range specified by user.

The graph shows that both the curves are running simultaneously in the range of $x = 0\ mm\ and\ x = 50mm$ and can't be seen separately as NURBS surface, object file or original surface deviation. Even for the smaller span of 24.5 mm and 25.5 mm the curves are unrecognized. They are exactly superimposed. Therefore, with the acceptance of 30 microns surface finish error one can expect similar results whether it is ray traced results on NURBS surface or with obj and original surface deviation. It can be seen that there exists no deviation. From Fig. 4.9-4.12, the red colour indicated FFRNS, blue colour indicates FFOBJS and green colour indicates FFSTLS.

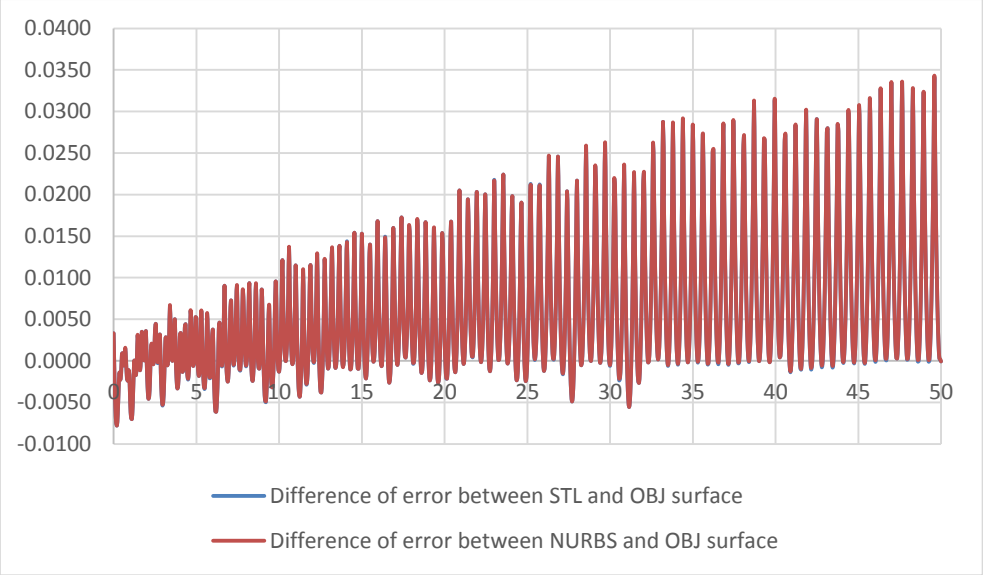

(a)

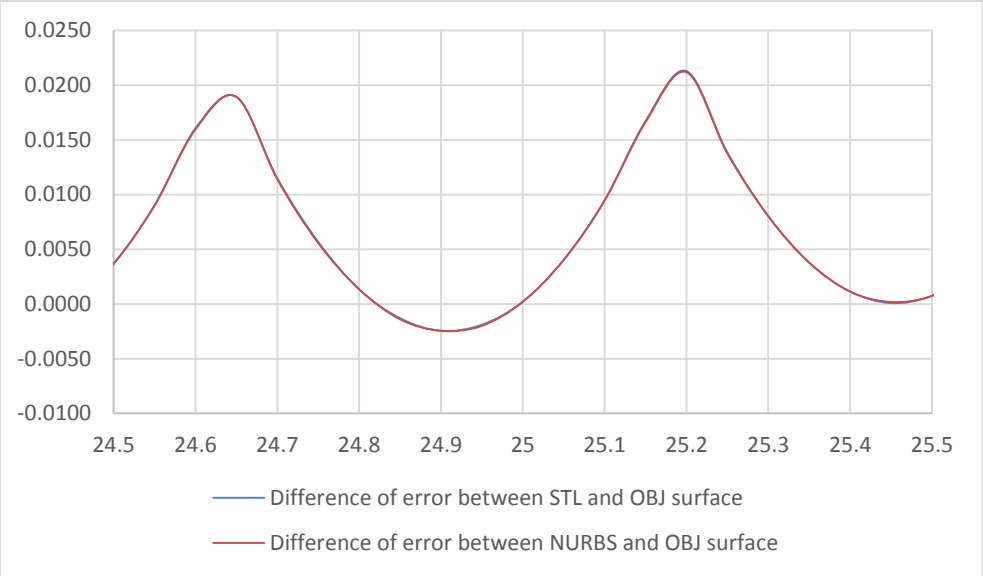

(b)

Figure 4.9: Difference of error between surface profile curves generated using ray tracing on NURBS and STL surface with respect to OBJ surface for a span of (a)50 mm and (b) 1mm from x = 24.5 to x = 25.5.

Figure 4.10 shows the plots for the absolute ray traced value for NURBS STL with $UV = 0.01$ which is the approximation of the actual surface, freeform NURBS STL with discretization level $UV = 0.025$ and for the obj data.

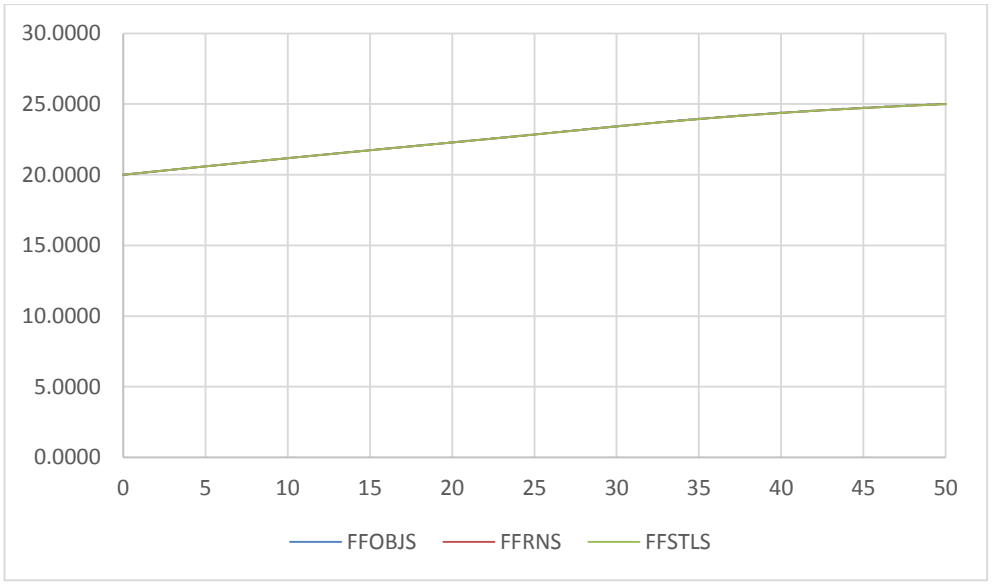

(a)

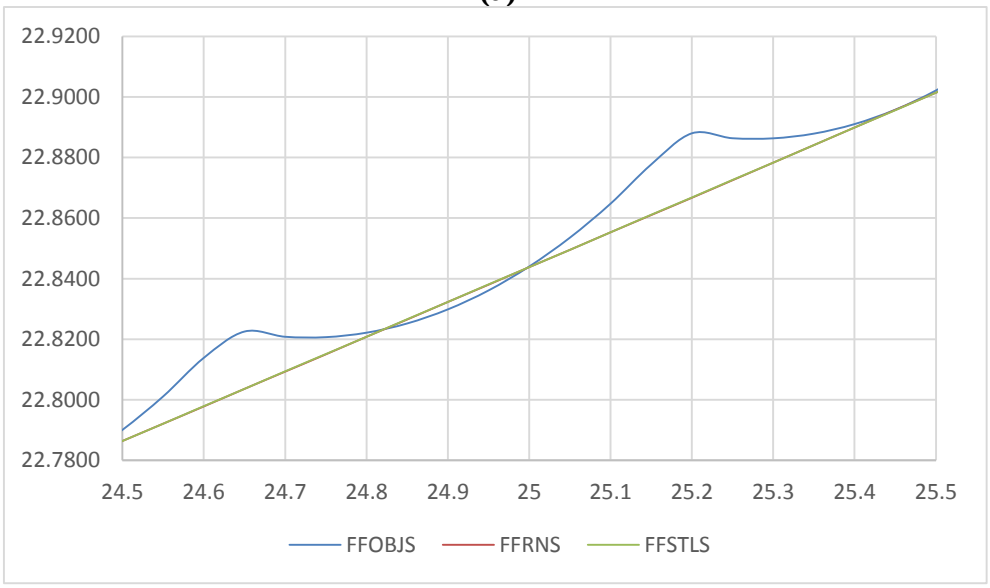

(b)

Figure 4.10: Reference surface profile curve (z heights) for $y = 25mm$ location plotted for a span of (a) 50 mm and (b) 1mm from x = 24.5 to x = 25.5.

It is observed from Fig. 4.10 (a) that there is no clear demarcation between the curves FFSTLS, FFOBJS and FFRNS but definitely it has got an error of 35 microns. To observe clear separation, the range of side step is taken for $x = 24.5\ mm\ to\ x = 25.\ mm$. The FFOBJS and FFSTLS can be seen clearly in the band of 24.5 mm and 25.5 mm. It is observed that FFRNS and FFSTLS overlap each other but FFOBJS lies right upside the FFRNS and FFSTLS curves which show that the tool penetration did not take place.

The similar exercise is done for freeform NURBS surface where the comparison is shown between reference NURBS curve for all values of x at $y = 15\ mm$, the STL with $UV = 0.025$ discretization level and the object file data obtained from graphical simulation.

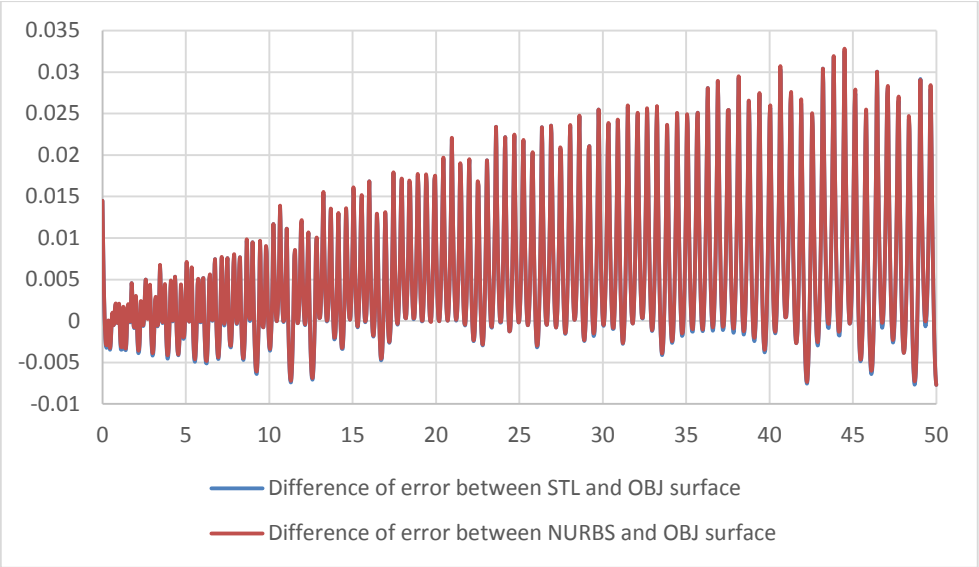

(a)

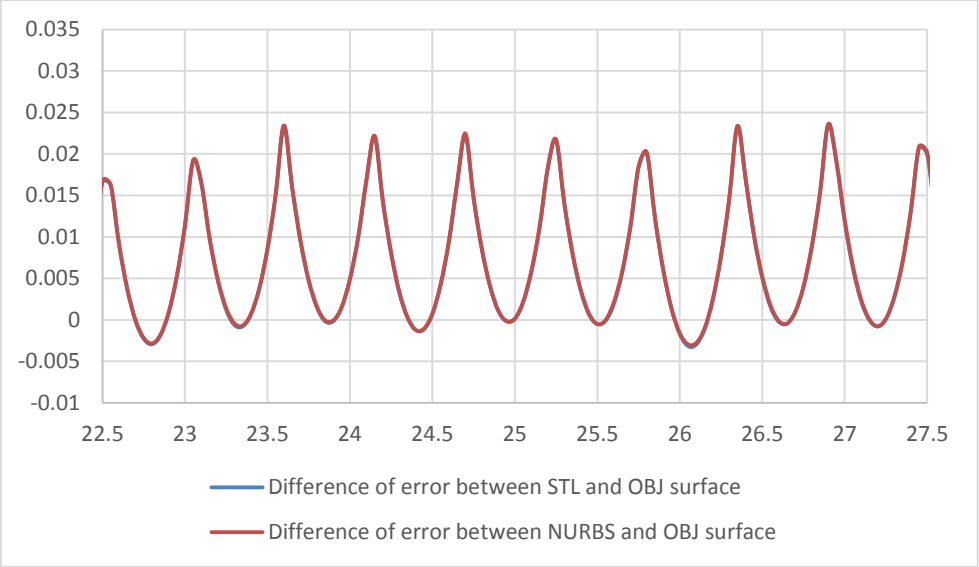

(b)

Figure 4.11: Difference of error between surface profile curves generated using ray tracing on NURBS and STL surface with respect to OBJ surface for a span of (a) 50 mm and (b) 1mm from x = 24.5 to x = 25.5.

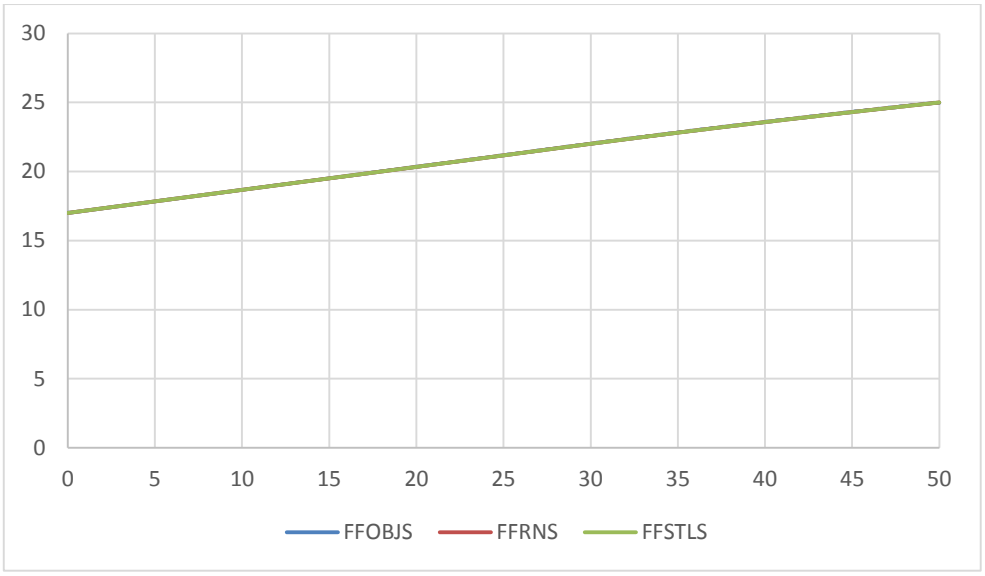

(a)

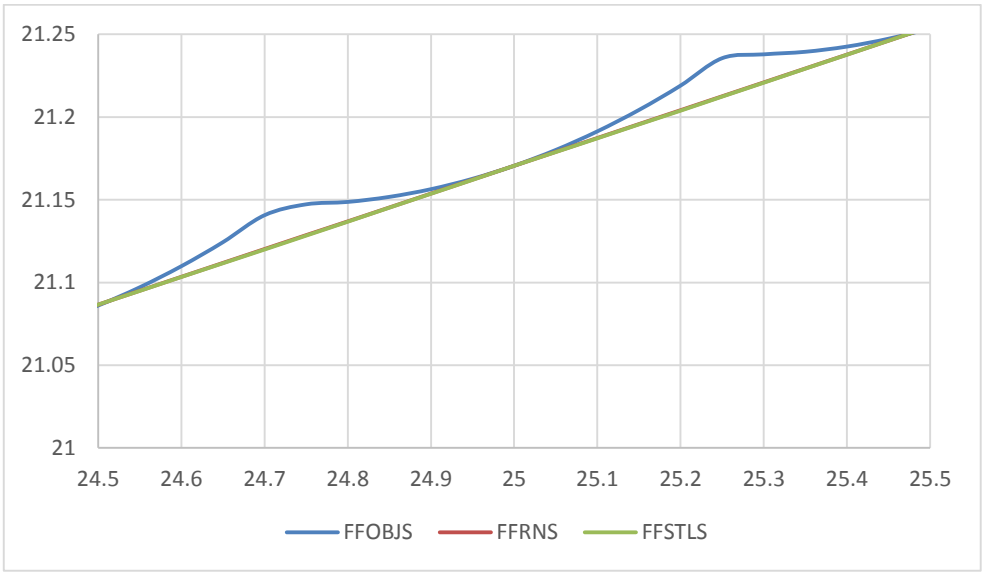

(b)

Figure 4.12: Reference surface profile curve (z heights) for $y = 15mm$ location plotted for a span of (a) 50 mm and (b) 1 mm from x = 24.5 to x = 25.5.

Figure 4.11 shows that the surface error is within the permissible range whereas Fig. 4.12 depicts that the two curves FFRNS and FFSTLS follow each other. The FFOBJS represents the machine profile deviation, is upside at three places while the lower side deviation with respect to FFSTLS of 0.02 mm occurs only at two places, which may be pertaining to simulation and approximation errors of graphical simulator.

4.4.2 Concave NURBS surface

The similar exercise is done for concave NURBS surface for which the plots are shown. Figure 4.13 are the plots for the differences in error for surface profile curve generated by using ray tracing on NURBS surface (triangulated with discretization level of 0.01) and STL surface with discretization level $UV = 0.0250$ taken with respect to the object surface generated from ToolSim graphical simulator.

Figure 4.13(a) shows the full band of side step distance ranging from $x = 0\ to\ x = 50mm$ and Figure 4.13(b) shows the range of x from 22.5 mm to 27.5 mm. It is clear from the profile curves, that surface error feed direction algorithm is around 35 micron but for middle portion, algorithm has achieved the surface error within the permissible limit. It can be seen that there exists no deviation. In Fig. 4.13-4.16, the red colour indicated CCRNS, blue colour indicates CCOBJS and green colour indicates CCSTLS.

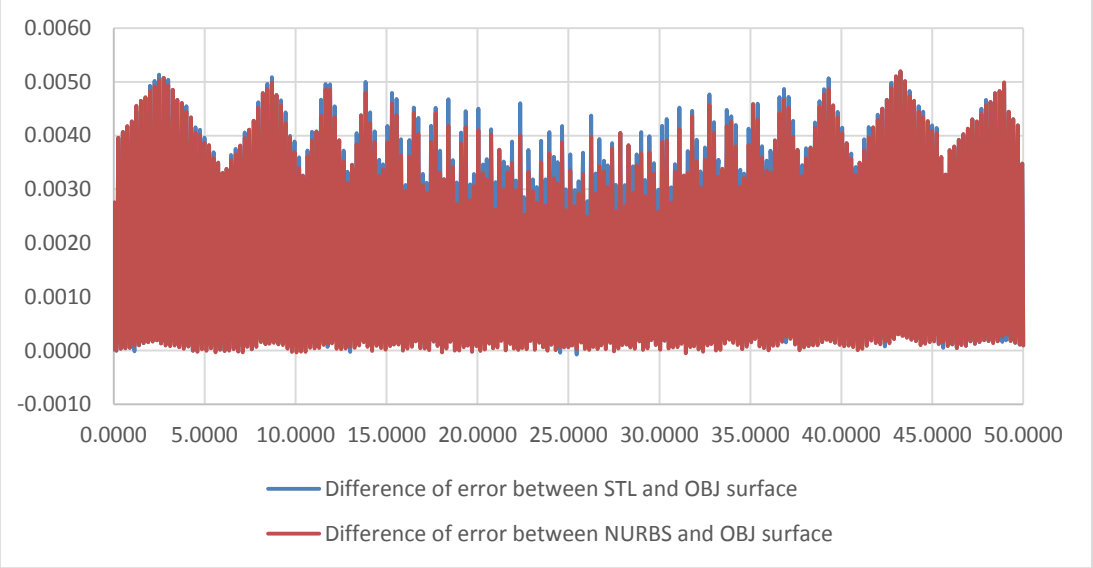

(a)

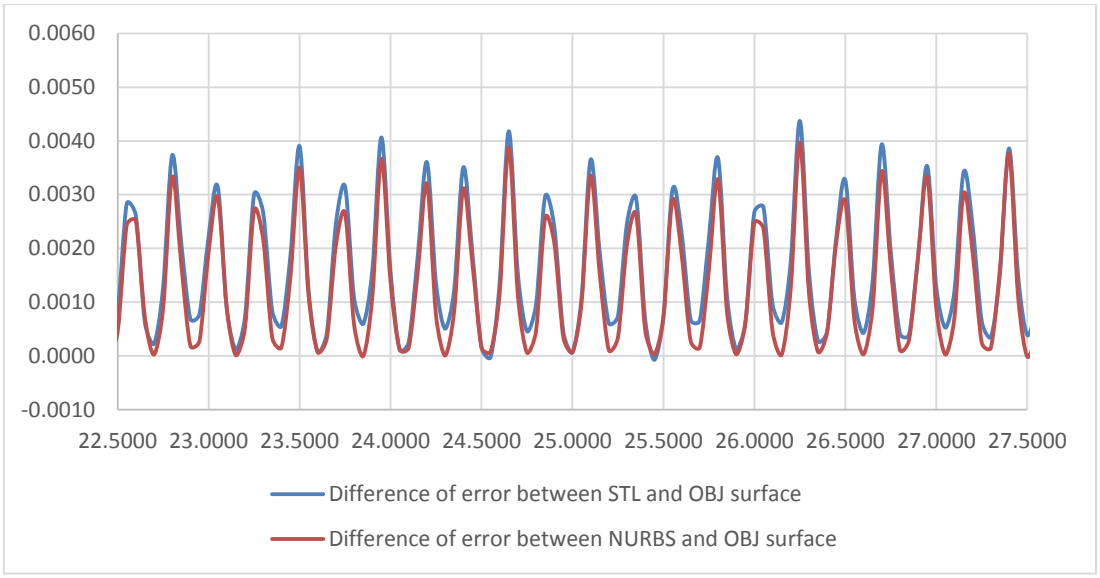

(b)

Figure 4.13: Difference of error between surface profile curves generated using ray tracing on NURBS and STL surface with respect to OBJ surface for a span of (a) 50 mm and (b) 1mm from x = 22.5 to x = 27.5

The reference surface profile curve (z heights) for given $y = 25\ mm$ location of workpiece plotted for a range of x-axis is plotted for the concave surface with 0.025 UV discretization level. The graphs shown in Fig 4.14(b) represents that the CCOBJ curve runs above the CCSTLS which shows the tool does not gouge the surface.

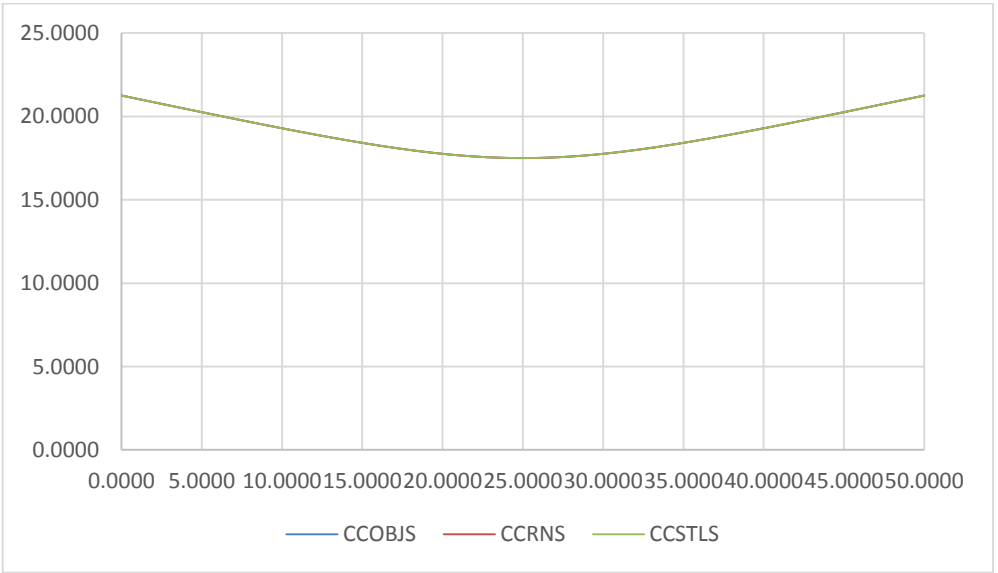

(a)

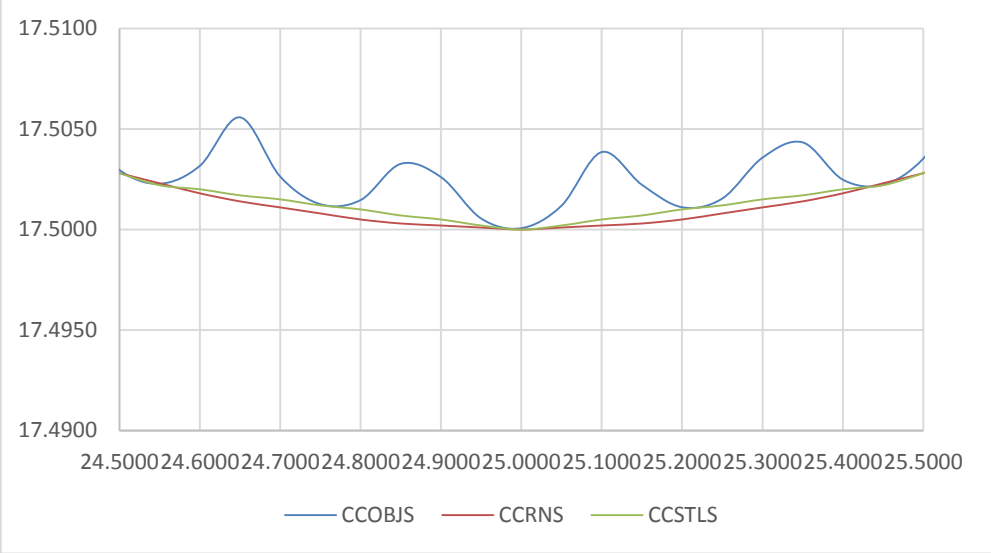

(b)

Figure 4.14: Reference surface profile curve (z heights) for $y = 25$ mm location plotted for a span of (a) 50 mm and (b) 1mm from x = 24.5 to x = 25.5.

The similar exercise is done for concave NURBS surface where the comparison is shown between reference NURBS curve for all values of x at $y = 15\,mm$, the STL with $UV = 0.025$ discretization level and the object file data obtained from graphical simulation.

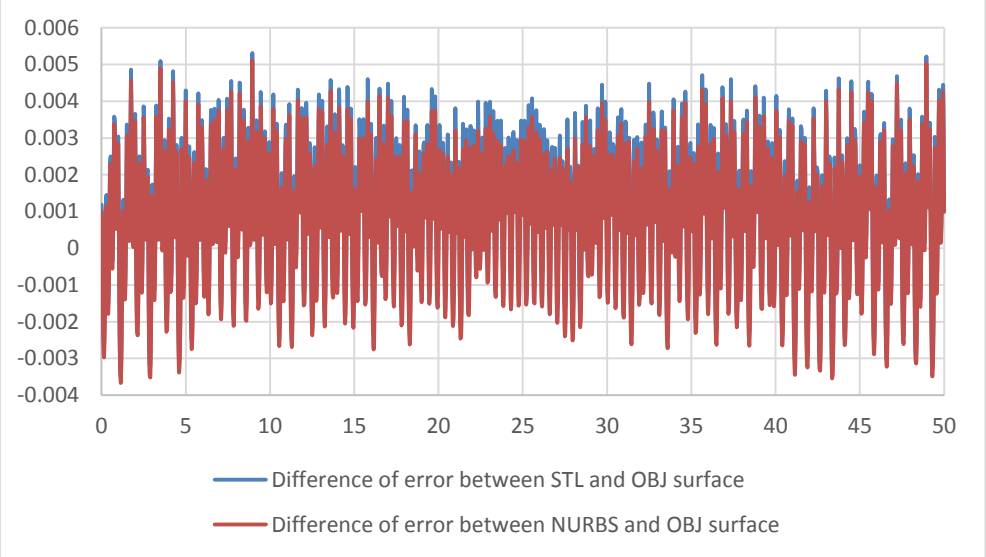

(a)

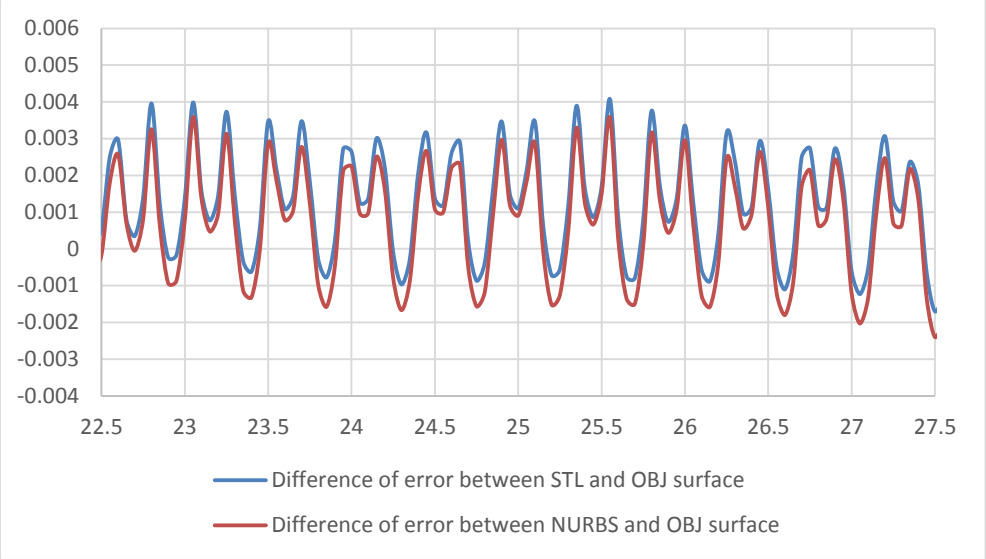

(b)

Figure 4.15: Difference of error between surface profile curves generated using ray tracing on NURBS and STL surface with respect to obj surface for a span of (a) 50 mm and (b) 5 mm

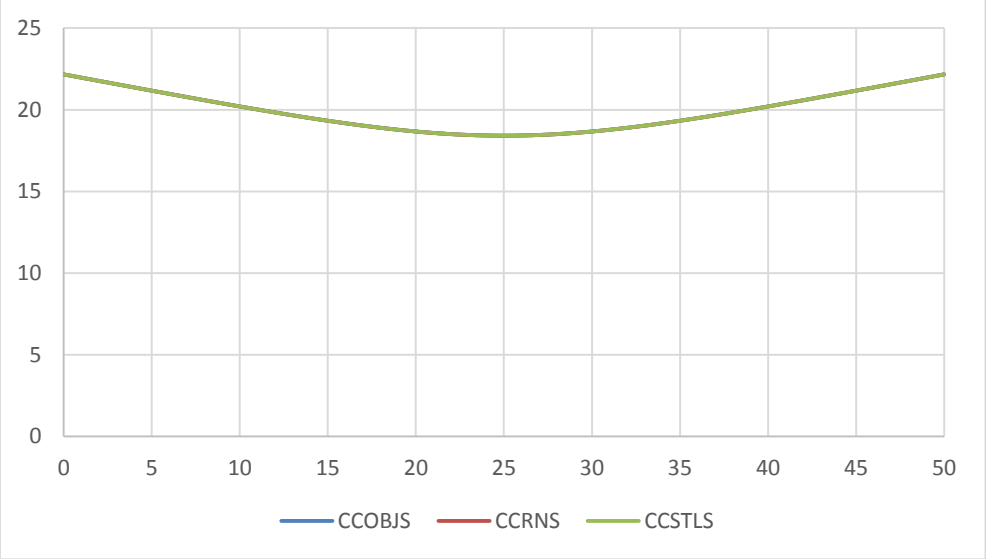

(a)

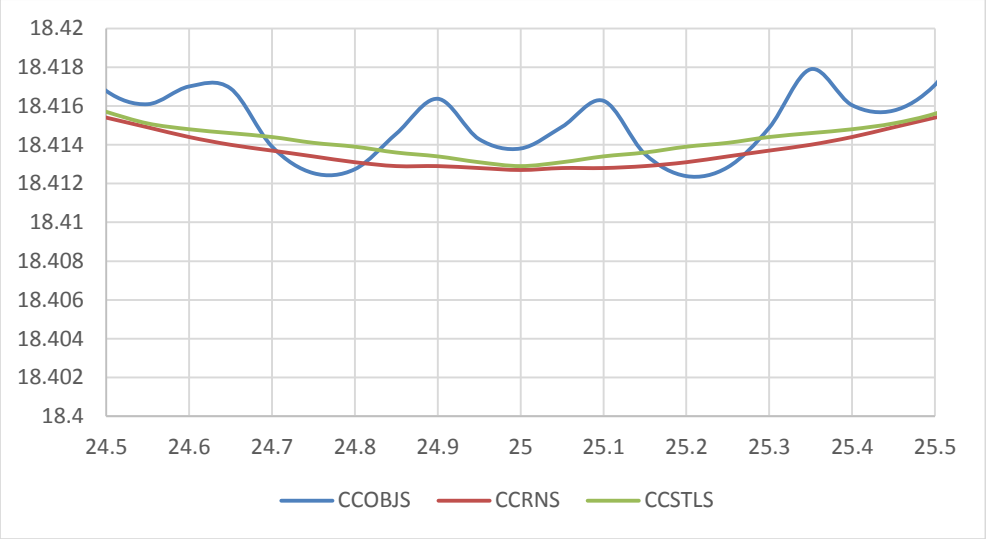

(b)

Figure 4.16: Reference surface profile curve (z heights) for $y = 15$ mm location plotted for a span of (a) 50 mm and (b) 1 mm from x = 24.5 to x = 25.5.

It is observed from Fig. 4.16 that the CCOBJS is well above the CCSTLS but at two places the deviation in the negative side is observed about 2 microns which may be due to the approximation of the graphical simulator.

4.4.3 Convex NURBS surface

The similar exercise is repeated for convex NURBS surface with discretization level of $UV = 0.025$. Figure 4.17 represents the plots for the differences in error for surface profile curve generated by using ray tracing on NURBS surface (triangulated with discretization level of 0.01) and STL surface with discretization level $UV = 0.025$ taken with respect to the object surface generated from ToolSim graphical simulator.

The surface errors graphs shows that for the span of 50 mm, the height of the scallops encountered is approximately 35 microns at the start and at the end but, when observed for the middle area i.e. for $x = 24.5\ mm\ to\ x = 25.5\ mm$, the scallop height found is within the range of user defined value as shown in the graph below in Fig. 4.17. In Fig. 4.17-4.20, the CVRNS is indicated by red, CVOBJS by blue and CVSTLS by green.

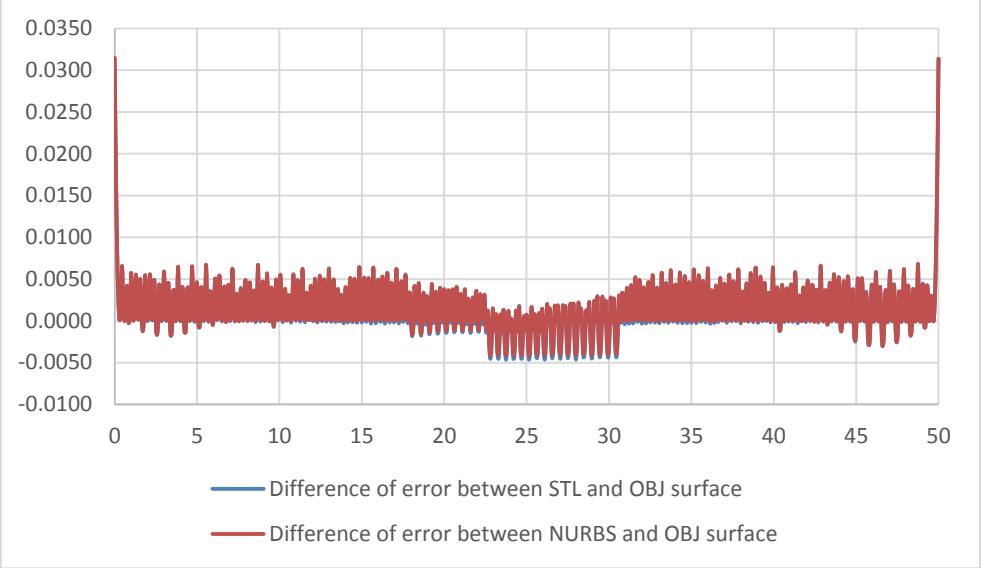

(a)

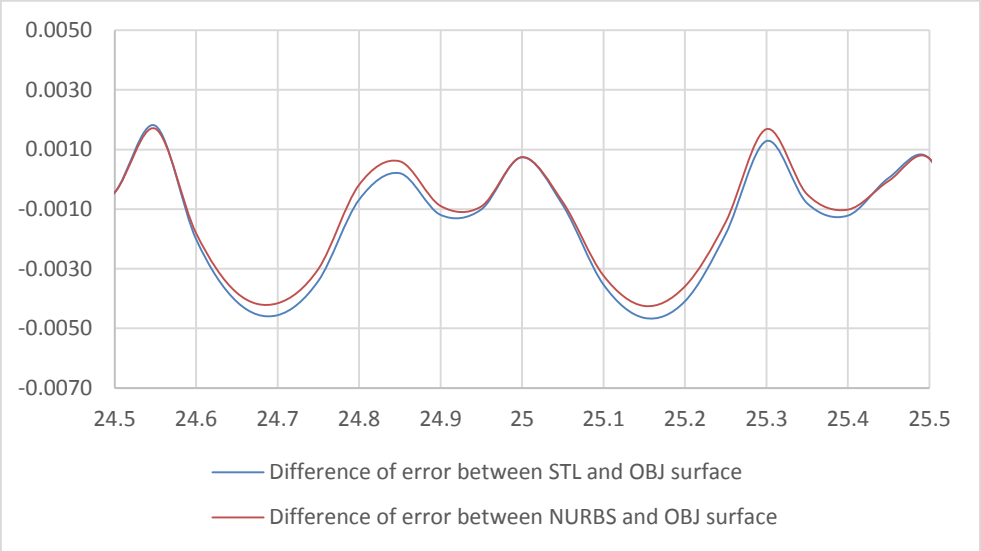

(b)

Figure 4.17: Difference of error between surface profile curves generated using ray tracing on NURBS and STL surface with respect to obj surface for a span of (a) 50 mm and (b) 1 mm from x = 24.5 to x = 25.5.

Now, an attempt is made to show the closeness of the curves on actual surface without taking the deviation. The reference surface profile curve (z heights) for given $y = 25\ mm$ location of workpiece plotted for a range of x-axis is plotted for the concave surface with 0.025 UV discretization level.

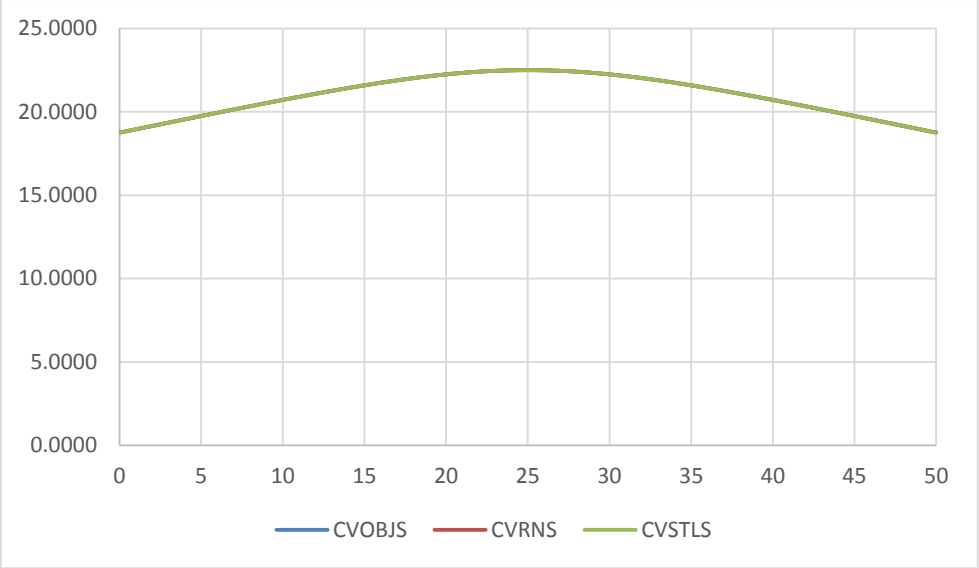

(a)

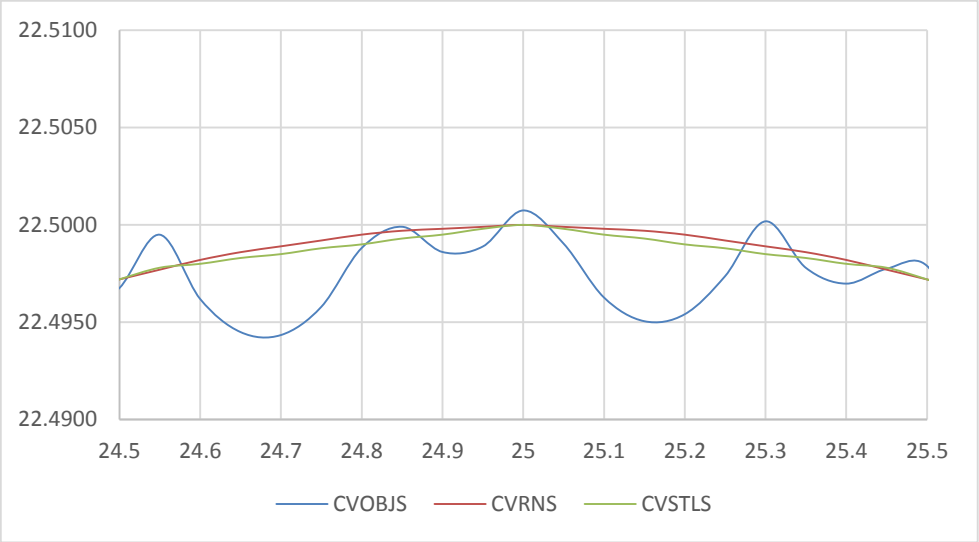

(b)

Figure 4.18: Reference surface profile curve (z heights) for $y = 25$ mm location plotted for a span of (a) 50 mm and (b) 1mm from x = 24.5 to x = 25.5.

The graph shown in Fig. 4.18 depicts that the CVOBJS is above the CVSTLS and CVRNS for the entire span of 50 mm but in the middle region where value of x is in between 24.5 mm and 25.5 mm there is a deviation below the CVSTLS and CVRNS of approximately 5 microns due to the approximation error by the graphical simulator.

The similar exercise is done for convex NURBS surface where the comparison is shown between reference NURBS curve for all values of x at $y = 15$ mm, the STL with $UV = 0.025$ discretization level and the object file data obtained from graphical simulation.

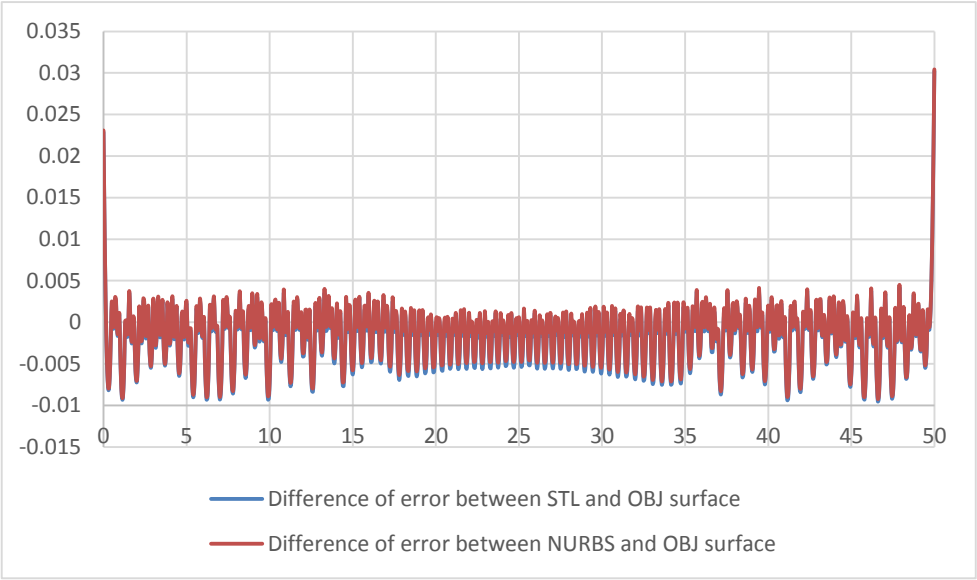

(a)

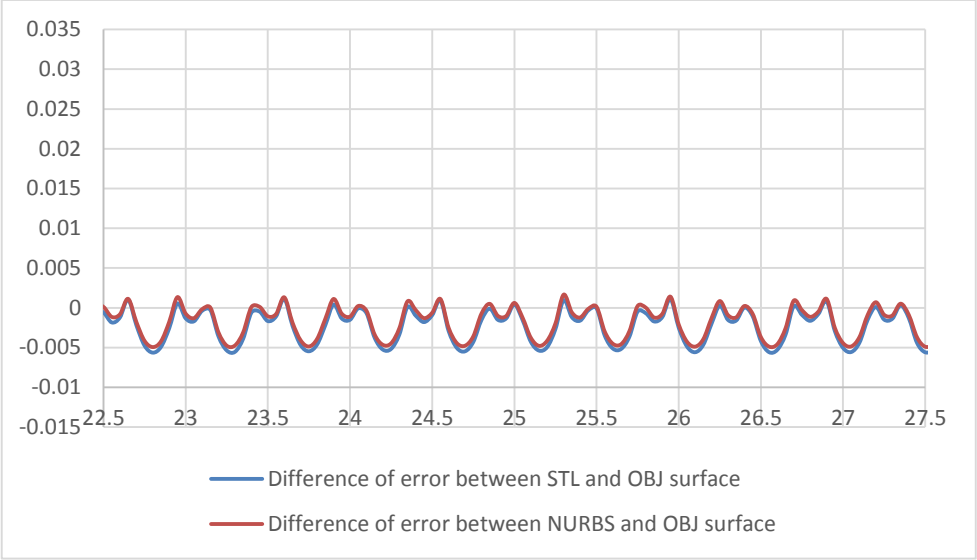

(b)

Figure 4.19: Difference of error between surface profile curves generated using ray tracing on NURBS and STL surface with respect to OBJ surface for a span of (a) 50 mm and (b) 5 mm.

Now, an attempt is made to show the closeness of the curves on actual surface without taking the deviation. The reference surface profile curve (z heights) for given $y = 15$ mm location of workpiece plotted for a range of x-axis is plotted for the concave surface with 0.025 UV discretization level.

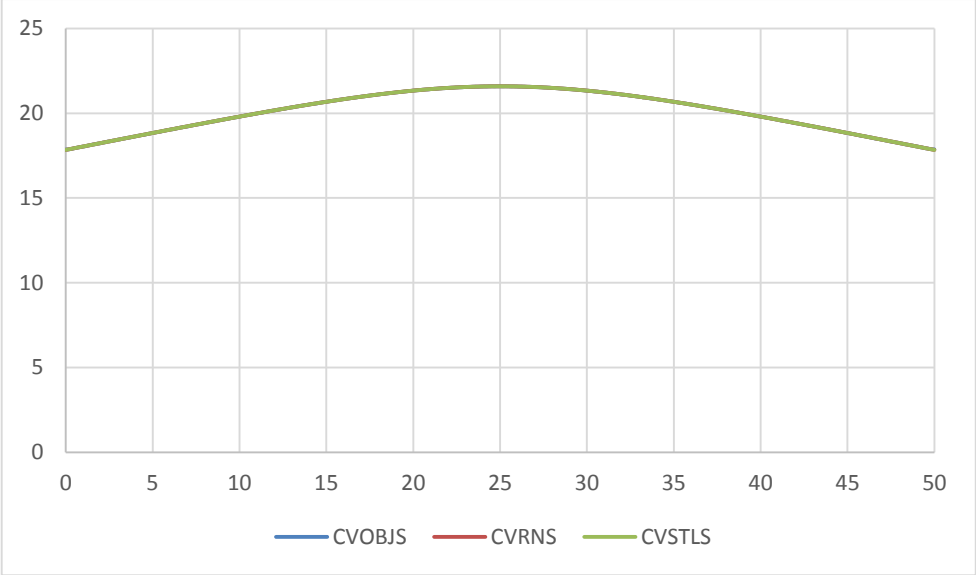

(a)

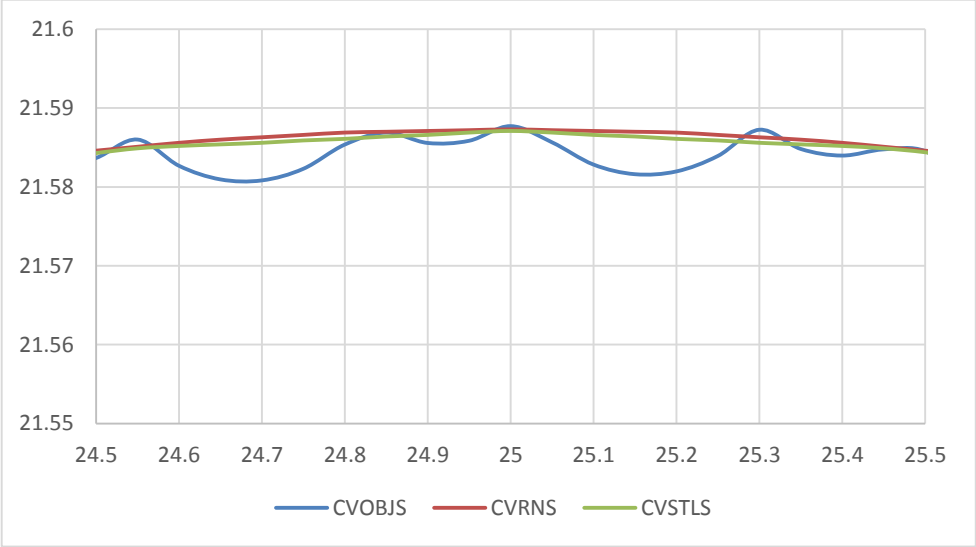

(b)

Figure 4.20: Reference surface profile curve (z heights) for $y = 15$ mm location plotted for a span of (a) 50 mm and (b) 1 mm from x = 24.5 to x = 25.5.

The CVOBJS runs in the lower side of CVRSTL and CVRNS as shown in Fig 4.20(b). This error may again pertain to the approximation of these curves in the central position as well as because of the higher value of feed forward distance.

4.5 Conclusion

The diameter of radius has great influence on minimum achievable scallop height. In this case iso-parametric discretization level of $UV = 0.025$ is taken for freeform NURBS, concave NURBS and convex NURBS surface. The minimum value of scallop height observed is 0.035

mm and this trend is consistent and it does not have any effect on minima achieved on scallop height.

From the surface error plots as shown in Fig. 4.9, 4.11, 4.13, 4.15, 4.17and 4.19 it is observed that the difference of error with respect to NURBS surface, with respect to freeform, concave and convex not seen much in terms of magnitude. The difference with the magnitude is in terms of 0.3 microns on an average but if we see the results with respect to the plot of the ray traced reference surface curves on reference NURBS surface as well as the input STL file with minimum value of iso-parametric discretization level ($UV = 0.025$). It has been seen that these three profile are almost in the similar position and simultaneously the surface profile obtained from graphical simulator which is represented as FFOBJS , CCOBJS and CVOBJS as shown in Fig. 4.10, 4.12, 4.14, 4.16, 4.18 and 4.20. It has been observed that these profiles are upside of their respective reference NURBS surface and reference STL surface. The object file curve at some positions is coming little downward with marginal error. This may pertain due to computational errors as well as because of graphical simulation errors.

Chapter 5 Conclusions and Future Scope

In this dissertation work, an algorithm for NC toolpath generation for a triangulated NURBS surface machined with a ball end milling cutter is presented. The developed C++ program based on the mathematical model presented in chapter 3 is used for toolpath generation for various triangulated models for freeform, concave and a convex NURBS surfaces with varying iso-parametric discretization. These meshed models were machined in a custom developed Open GL based graphical simulator ToolSim and the machined model data is captured in the form of point cloud data which is further compared with a reference surface profile curves generated from the corresponding meshed input surface model for toolpath generation. The reference part surface profiles for comparison are generated from the corresponding meshed model using a ray tracing program. Further a simulation study has been conducted to find the effect of tool radius and iso-parametric mesh spacing on surface finish. The detailed results are presented in the chapter 5. In this section the conclusions drawn from the present study is presented along with the future scope.

5.1 Conclusions

The conclusions drawn from the present study are as follows:

i. The iso-parametric discretization used for meshing of the NURBS surface does not affect the surface finish achievable within the limit of machining the total surface with a nominal number of machining passes.

ii. The study shows that the smaller radius ball end cutter helps in achieving better surface finish levels without significantly increasing the number of machining passes.

iii. For a given tool dimensions and the given meshed part surface, the comparison of ray traced surface profile with the curve on the graphically simulated machined part shows that for a given cross-section the toolpath data ensures the minimum specified scallop height.

iv. As seen from surface error results for concave and convex surfaces, the tool positions at beginning and as well as at the end accounts for higher scallop height as compared to middle region where the scallop height is obtained in the region from -0.005 microns to 2 microns but the overall strategy gives the result for 35 microns. So, for better insights of results, local subdivisions of region would have been better and adaptive side steps

values may be planned where the regions with tool entry points into the machined surface can be accepted with higher surface finish tolerance when compared to inner values where the smaller surface tolerances can be specified.

v. The side steps value encountered in toolpath generation for freeform, concave and convex NURBS shapes are observed reasonable as they are neither too close nor too far. Hence, controlled scallop toolpath algorithm is able to adjust the required toolpath according to maximum permissible value of scallop height suggested.

5.2 Future Scope of Work

i. The effect of other tool shapes like flat, radiused or conical end mills can be considered for this study.

ii. The detailed study can be conducted to identify the effect of curvature change on a sculptured NURBS surface and the effect of scallop height for a given tool dimensions.

iii. The ideal simulations results from the graphical simulations can be compared with the actual machining results.

iv. This dissertation work can be extended for composite sculptured surfaces having concave, convex and transition regions.

v. The toolpath pattern other that zig-zag pattern can also be used where local subdivision of triangulated composite sculptured surface can be used to identify in a better way the behavior of the controlled scallop height algorithm and the tool size required to achieve that value and the number of machining passed required for that local region.

Annexure-(A)

A.1 Detailed data of scallop height tool radius and iso- parametric discretization of triangulated NURBS surface

The table A.1 shows the detailed data of the relationship between tool radius, scallop height achievable and iso-parametric discretization of triangulated NURBS surface at different levels. The summary of the data presented in the table A.1 is shown in Table 4.5 of chapter 4. The Table A.1 is shown below..

Table A.1: Detailed data for scallop height, tool radius and iso- parametric discretization of triangulated NURBS surface

								Radius of Ball End Mill (mm)											
								1.5875				3.175				6.35			
Shape of the NURBS surface	U-V discritization	Total number of facetes on the Surface	Total area of surface	Facet density (facets per mm square)	Average area per facet	Minimum facet area	Maximum facet area	Scallop height (mm)	Total number of toolpaths required	Total number of tool positions	Processing Time (sec)	Scallop height (mm)	Total number of toolpaths required	Total number of tool positions	Processing Time (sec)	Scallop height (mm)	Total number of toolpaths required	Total number of tool positions	Processing Time (sec)
Concave Surface	0.025	12800	2563.455	4.993261048	0.200269922	0.19889	0.445456	0.030	Excessive toolpaths encounted			0.060	Excessive toolpaths encounted			0.125	Excessive toolpaths encountered		
								0.035	211	10761	355.58	0.065	159	8109	615.482	0.130	83	4233	251.297
								0.040	147	7497	240.301	0.070	107	5457	392.055	0.135	65	3315	156.740
								0.045	119	6069	197.308	0.070	107	5457	168.351	0.140	57	2907	145.559
	0.050	3200	2563.437	1.248324027	0.801074063	0.440247	1.738003	0.030	Excessive toolpaths encounted			0.060	Excessive toolpaths encounted			0.125	Excessive toolpaths encounted		
								0.035	89	4539	159.268	0.065	133	6783	48.157	0.130	83	4233	31.548
								0.040	131	6681	126.343	0.070	99	5049	33.786	0.135	65	3315	20.320
								0.045	111	5661	108.037	0.075	83	4233	26.508	0.140	57	2907	12.847
	0.075	1352	2378.085	0.568524674	1.758938609	0.989988	3.814899	0.030	Excessive toolpaths encounted			0.060	Excessive toolpaths encounted			0.125	Excessive toolpaths encounted		
								0.035	179	8771	32.39	0.065	127	6477	25.857	0.130	55	2695	13.5
								0.040	135	6615	26.008	0.070	97	4753	17.861	0.135	83	4233	8.62
								0.045	111	5439	21.212	0.075	83	4067	12.751	0.140	63	3087	5.444
	0.100	800	2563.365	0.312089773	3.20420625	0.033261	0.072342	0.030	Excessive toolpaths encounted			0.060	Excessive toolpaths encounted			0.125	Excessive toolpaths encounted		
								0.035	157	8007	41.801	0.065	115	5865	19.944	0.130	75	3825	16.986
								0.040	127	6477	34.219	0.070	91	4641	13.811	0.135	61	3111	10.937
								0.045	109	5559	29.716	0.075	79	4029	12.632	0.140	55	2805	7.234
Convex Surface	0.025	12800	2563.455	4.993261048	0.200269922	0.109889	0.445456	0.030	Excessive toolpaths encounted			0.060	Excessive toolpaths encounted			0.125	Excessive toolpaths encounted		
								0.035	189	9639	295.307	0.065	161	8211	268.227	0.130	83	4233	138.194
								0.040	141	7191	222.803	0.070	107	5457	173.053	0.135	65	3315	96.461
								0.045	117	5967	190.293	0.075	81	3969	135.992	0.140	55	2805	51.410
	0.050	3200	2563.437	1.248324027	0.801074063	0.440247	1.738003	0.030	Excessive toolpaths encounted			0.060	Excessive toolpaths encounted			0.125	Excessive toolpaths encounted		
								0.035	187	9537	186.481	0.065	73	3723	68.373	0.130	79	4029	33.145
								0.040	139	7089	136.83	0.070	105	5355	43.176	0.135	61	3111	19.121
								0.045	115	5865	112.409	0.075	85	4335	33.923	0.140	53	2703	10.770
	0.075	1352	2378.085	0.568524674	1.758938609	0.989988	3.814899	0.030	Excessive toolpaths encounted			0.060	Excessive toolpaths encounted			0.125	Excessive toolpaths encounted		
								0.035	165	8085	71.817	0.065	143	7007	31.557	0.130	71	3479	10.987
								0.040	127	6223	57.43	0.070	99	4851	24.07	0.135	57	2793	7.077
								0.045	107	5243	45.983	0.075	81	3969	19.12	0.140	49	2499	4.135
	0.100	800	2563.365	0.312089773	3.20420625	0.33261	0.072342	0.030	Excessive toolpaths encounted			0.060	Excessive toolpaths encounted			0.125	Excessive toolpsths encounted		
								0.035	143	7293	16.442	0.065	155	7905	14.921	0.130	65	3315	4.857
								0.040	113	5763	12.711	0.070	105	5355	9.082	0.135	55	2805	2.985
								0.045	99	5049	11.666	0.075	85	4335	7.001	0.140	53	2703	2.293
Freeform Surface	0.025	12800	2533.631	5.052037964	0.197939922	0.111314	0.445198	0.030	Excessive toolpaths encounted			0.060	Excessive toolpaths encounted			0.120	Excessive toolpaths encounted		
								0.035	105	5355	180.627	0.065	63	3213	67.449	0.125	55	2805	44.650
								0.040	91	4641	159.763	0.070	59	3009	55.033	0.130	53	2703	35.421
								0.045	83	4233	140.334	0.075	55	2805	43.025	0.135	53	2703	32.053
	0.050	3200	2533.64	1.263005005	0.7917625	0.442681	8.973197	0.030	Excessive toolpaths encounted			0.060	Excessive toolpaths encounted			0.125	Excessive toolpaths encounted		
								0.035	105	5355	43.411	0.065	63	3213	17.488	0.130	53	2703	22.272
								0.040	83	4233	40.025	0.070	59	3009	13.227	0.135	53	2703	21.120
								0.045	93	4743	37.866	0.075	55	2805	10.39	0.140	55	2805	19.804
	0.075	1352	2353.308	0.574510434	1.740612426	1.002825	3.180916	0.030	Excessive toolpaths encounted			0.060	Excessive toolpaths encounted			0.120	Excessive toolpaths encounted		
								0.035	103	5047	17.764	0.065	63	3087	6.94	0.125	61	2989	7.938
								0.040	89	4361	15.211	0.070	57	2793	4.414	0.130	53	2597	4.180
								0.045	81	3969	14.414	0.075	55	2695	3.997	0.135	49	2499	3.701
	0.100	800	2533.675	0.315746889	3.16709375	0.017808	0.072328	0.030	Excessive toolpaths encounted			0.060	Excessive toolpaths encounted			0.125	Excessive toolpaths encounted		
								0.035	105	5355	8.311	0.065	67	3417	6.945	0.130	57	2907	7.155
								0.040	91	4641	5.7124	0.070	59	3009	4.86	0.135	55	2805	5.510
								0.045	83	4233	8.241	0.075	57	2907	2.165	0.140	55	2805	5.420

References

[1] Lai, J.Y., & Wang, D. J. (1994). A strategy for finish cutting path generation of compound surfaces. *Computers in Industry*, 25, 189–209.

[2] Lin, C. Y., Hwang, Y. Y., & Lai, J. Y. (1997). Interference-Free Cutting-Path Generation Based on Scanning Data. *The International Journal of Advanced Manufacturing Technology*, 13, 535–547.

[3] Hwang, J. S., & Chan, T. C. (1998). Three-axis machining of compound surfaces using flat and filleted end mills. *Computer-Aided Design*, 30, 641–647.

[4] Lin, A.C., & Liu, H. T. (1998). *Automatic generation of NC cutter path from massive data points*. *Computer- Aided Design*, 30, 77–90.

[5] Feng, H.Y., & Li, H. (2002). Constant scallop-height tool path generation for three-axis sculptured surface machining. *Computer Aided Design*, 34, 647–654.

[6] Kim, B.H., & Choi, B.K. (2002). Guide surface based tool path generation in 3-axis milling: an extension of the guide plane method. *Computer-Aided Design*, 32, 192–199.

[7] Kim, B.H., and Choi, B.K. (2002). Machining efficiency comparison direction – parallel tool path with contour –parallel tool path. *Computer-Aided Design*, 34, 89–95.

[8] Park, S. C. (2004). Sculptured surface machining using triangular mesh slicing. *Computer-Aided Design*, 36, 279–288.

[9] Ren, Y., Zhu W., & Lee, Y. S. (2004) Material side tracing and curve refinement for pencil-cut machining of complex polyhedral models. *Computer-Aided Design*, 37, 1015–1026.

[10] Yau, H.T., Chuang, C.M., & Lee, Y.S. (2004). Numerical control machining of triangulated sculptured surfaces in a stereo lithography format with a generalized cutter. *International Journal of Production Research*, 42, 2573–2598.

[11] Lee, D. Y., Kim, S. J., Kim, H. C., Lee, S.G., & Yang, M.Y. (2006). *Incomplete two-manifold mesh-based tool path generation. The International Journal Of Advanced Manufacturing Technology*, 27, 797–803.

[12] Teng. Z., Feng. H.Y., & Azeem, A. (2006). Generating efficient tool paths from point cloud data via machining area segmentation. *International Journal of Advanced Manufacturing Technology*, 30, 254–260.

[13] Yuwen, S., Dongming, G., & Haixia, W. (2006). Iso-parametric tool path generation from triangular meshes for free-form surface machining. *The International Journal of Advanced manufacturing Technology*, 28, 721–726.

[14] Manos, N.P., Bedi, S., Miller, D., & Mann, S. (2007). Single controlled axis lathe mill. *The International Journal of Advanced Manufacturing Technology*, 32, 55-65.

[15] Chen, T., & Shi, Z. (2008). A tool path generation strategy for three-axis ball-end milling of free-form surfaces. *journal of materials processing technology*, 208, 259–263

[16] Lee, S.G., Kim, H.C., & Yang, M.Y. (2008). Mesh-based tool path generation for constant scallop-height machining. *The International Journal Of Advanced Manufacturing Technology*, (2008), 37, 15–22.

[17] Makki, M., Lartigue, C., & Thiébaut, F.(2008).Direct duplication of physical models in discrete 5-axis machining. *Virtual and Physical Prototyping*, 3, 93-103.

[18] Yang, D. O., & Feng, H. Y. (2008). Machining Triangular Mesh Surfaces via mesh offset based tool paths. *Computer-Aided Design and Applications*, 5, 254–265.

[19] Jasra, P.M. (2009). *Generalized tool path generation algorithm for sculptured pseudo symmetric surface machining* (M.E. dissertation, Thapar University Patiala).

[20] Kayal, P. (2009). Inverse offset method for adaptive cutter path generation from point-based surface. *International journal of CAD/CAM*, 7, 203-214.

[21] Zhang, D., Yang, P., and Qian, X. (2009). Adaptive NC path generation from massive point data with bounded error. *Journal of manufacturing science and engineering*, 131, 011001-1 –011001-13.

[22] Lasemi, A., Xue, D., & Gu, P. (2010). Recent development in CNC machining of freeform surfaces: A state-of-the-art review. *Computer-Aided Design*, 42, 641–654.

[23] Mann, S., Bedi, S., Israeli, G., & Zhou, X. L. (2010). Machine models and tool motions for simulating five-axis machining. *Computer –Aided Design*, 42, 231-237.

[24] Park, S. C., & Chang, M. (2010). Tool path generation for a surface model with defects. *Computers in Industry*, 61, 75-82.

[25] Patel, K., Bolaňos, G.S., Bassi, R., & Bedi, S. (2011). Optimal tool shape selection based on surface geometry for three-axis CNC machining. *The International Journal Of Advanced Manufacturing Technology*. 57, 655–670.

[26] Rajiv (2014). *Controlled scallop height tool path generation for 3-Axis vertical CNC machining of STL surfaces* (M.E. dissertation, Thapar University Patiala).

[27] Sortino, M., Belfio, S., Motyl, B., & Totis, G. (2014). Compensation of geometrical errors of CAM/CNC machined parts by means of 3D workpiece model adaptation. *Computer-Aided Design*, 48, 28–38.

[28] Duvedi, R.K., Bedi, S., Batish, A., & Mann, S. (2015). A multipoint method for machining of triangulated surface models. *The International Journal of Advanced Manufacturing Technology*, 52, 17-26.

Table 4.5: Detailed results for the minimum value of scallop height achieved by the tool for given value of ε

								Radius of Ball End Mill (mm)																	
								1.5875 mm						3.175 mm						6.35 mm					
Shape of the NURBS surface	Isoparameric (u-v) discritization	Total number of facetes on the Surface	Total area of surface	Facet density (facets per mm square)	Average area per facet	Minimum facet area	Maximum facet area	Minimum scallop height identified (mm)	Total number of toolpaths required	Total number of tool positions	Minimum side-step value achieved (mm)	Maximum side-step value achieved (mm)	Average side-step value achieved (mm)	Minimum scallop height identified (mm)	Total number of toolpaths required	Total number of tool positions	Minimum side-step value achieved (mm)	Maximum side-step value achieved (mm)	Average side-step value achieved (mm)	Minimum scallop height identified (mm)	Total number of toolpaths required	Total number of tool positions	Minimum side-step value achieved (mm)	Maximum side-step value achieved (mm)	Average side-step value achieved (mm)
Concave Surface	0.025	12800	2563.455	4.9933	0.2003	0.1989	0.4455	0.0350	211.0000	10761.0000	0.2133	0.4518	0.2392	0.0650	159.0000	8109.0000	0.2061	0.6254	0.3185	0.1300	83.0000	4233.0000	0.4448	1.0000	0.6098
	0.050	3200	2563.437	1.2483	0.8011	0.4402	1.7380	0.0350	89.0000	4539.0000	0.1747	0.4233	0.3030	0.0650	133.0000	6783.0000	0.2375	0.5541	0.3787	0.1300	83.0000	4233.0000	0.3229	1.0000	0.6173
	0.075	1352	2378.085	0.5685	1.7589	0.9900	3.8149	0.0350	179.0000	8771.0000	0.0446	0.4579	0.2722	0.0650	127.0000	6477.0000	0.2344	1.1301	0.3846	0.1300	55.0000	2695.0000	0.4448	1.0000	0.6098
	0.100	800	2563.365	0.3121	3.2042	0.0333	0.0723	0.0350	157.0000	8007.0000	0.2133	0.4518	0.2392	0.0650	115.0000	5865.0000	0.1733	0.8288	0.4424	0.1300	75.0000	3825.0000	0.0052	0.8102	0.6849
Convex Surface	0.025	12800	2563.455	4.9933	0.2003	0.1099	0.4455	0.0350	189.0000	9639.0000	0.2344	0.2904	0.2674	0.0650	161.0000	8211.0000	0.1430	0.3870	0.3167	0.1300	83.0000	4233.0000	0.5110	0.7037	0.6173
	0.050	3200	2563.437	1.2483	0.8011	0.4402	1.7380	0.0350	187.0000	9537.0000	0.2179	0.2932	0.2703	0.0650	73.0000	3723.0000	0.1483	0.3604	0.3247	0.1300	79.0000	4029.0000	0.5131	0.7464	0.6410
	0.075	1352	2378.085	0.5685	1.7589	0.9900	3.8149	0.0350	165.0000	8085.0000	0.2169	0.3254	0.2937	0.0650	143.0000	7007.0000	0.1620	0.3992	0.3392	0.1300	71.0000	3479.0000	0.2086	0.8464	0.6882
	0.100	800	2563.365	0.3121	3.2042	0.3326	0.0723	0.0350	143.0000	7293.0000	0.0613	0.4205	0.3546	0.0650	155.0000	7905.0000	0.1371	0.3929	0.3226	0.1300	65.0000	3315.0000	0.5924	0.9798	0.7937
Freeform Surface	0.025	12800	2533.631	5.0520	0.1979	0.1113	0.4452	0.0350	105.0000	5355.0000	0.1516	0.6599	0.4808	0.0650	63.0000	3213.0000	0.0001	1.0000	0.1161	0.1250	55.0000	2805.0000	0.0722	1.0000	0.9259
	0.050	3200	2533.640	1.2630	0.7918	0.4427	8.9732	0.0350	105.0000	5355.0000	0.2317	0.6622	0.4877	0.0650	63.0000	3213.0000	0.2527	1.0000	0.8065	0.1300	53.0000	2703.0000	0.4755	1.0000	0.9615
	0.075	1352	2353.308	0.5745	1.7406	1.0028	3.1809	0.0350	103.0000	5047.0000	0.2261	0.6502	0.4723	0.0650	63.0000	3087.0000	0.2416	1.0000	0.7770	0.1250	61.0000	2989.0000	0.0001	1.0000	0.8029
	0.100	800	2533.675	0.3157	3.1671	0.0178	0.0723	0.0350	105.0000	5355.0000	0.2316	0.6702	0.4808	0.0650	67.0000	3417.0000	0.2521	1.0000	0.7692	0.1300	57.0000	2907.0000	0.1160	1.0000	0.9091